POLITECNICO
MILANO 1863

Final degree project: **SpaceX's Raptor engine**

Authors:

Julian Ehrlich, Luca Frassinella, Nicolas Gaudenzi, Giacomo Marconcini, Pietro Mirri, Alessia Nardecchia, Edoardo Nicolucci Balocco, Samuele Orsenigo

AA: 2022-2023 – Course: Aerospace Propulsion

Professor: Luciano Galfetti

Student Code Table

Student code	Name and Surname	Student code	Name and Surname
10732773	*Julian Ehrlich*	10765536	*Pietro Mirri*
10795356	*Luca Frassinella*	10726866	*Alessia Nardecchia*
10764585	*Nicolas Gaudenzi*	10705062	*Edoardo Nicolucci Balocco*
10674321	*Giacomo Marconcini*	10735389	*Samuele Orsenigo*

Index

1 Introduction

In this paper we are going to analyse SpaceX's most ambitious engine: the Raptor which uses liquid methane to power his full flow stage combustion cycle.

Raptor is a prototype, and as such, it is constantly evolving. We have been closely monitoring its evolution, and that is why our study aims to focus on comparing Raptor with some of the best spacecraft engines. Our primary goal will be on describing and comparing (if possible) Raptor 1 and Raptor 2, considering both their similarities and differences. We will explore the reasons behind each design choice in both versions and analyze the motivations driving these decisions.

We divided ourselves into groups to better analyze and describe every aspect of the engine. We began the analysis by discussing the thrust chamber, followed by a close examination and comparison of the nozzles of Raptor 1 and Raptor 2, exploring the differences between the two solutions. After that, we decided to describe the cycle and its elements: the tanks, the turbopumps, the cooling jacket and the injectors.

Therefore, with the data coming up from the analysis, we wrote a final comparison to bring out the positive aspects of Raptor and why the SpaceX prototype can be considered the best engine for a spacecraft.

Now let's introduce SpaceX.

SpaceX is an American aerospace manufacturer and space transport services company with its headquarters in Hawthorne, California, USA. It designs, manufactures and launches the most advanced rockets and spacecraft in the world. The company was founded in 2002 by Elon Musk to revolutionize space transportation, with the ultimate goal of making life multiplanetary. In 2010, SpaceX became the first commercial company in history to send a spacecraft into orbit and return it safely to Earth. The company made history again in May 2012 when its Dragon spacecraft delivered cargo to and from the International Space Station, something previously accomplished only by governments.

The fact that SpaceX was the first commercial company to invest in space opened this world to a several number of companies who sees the space like an opportunity to grow and accomplish something that previously only the government could achieve.

The future of Raptor is bright: the goal is to increase efficiency and to make the engine simpler and lighter. One interesting design choice for this engine is the use of methane as fuel, which SpaceX has opted for. Designing the first stage, one of the most important things is the density of the propellant: with a denser fuel, the tanks can be smaller and lighter for a given mass of fuel and doing so a lighter rocket can be made.

	RP-1	METHANE	HYDROGEN
Density	813 g/L	422 g/L	70 g/L
Oxidizer : Fuel Ratio (as used)	2.7 : 1	3.7 : 1	6 : 1
1 Liter of LOX : X Liter of Fuel	1 : 0.52	1 : 0.73	1 : 2.7
Efficiency (Maximum Theoretical ISP)	370s	459s	532s
Combustion Temp	3670 K	3550 K	3070 K
Boiling Point	490 K	111 K	20 K
Combustion Byproducts	CO_2 & H_2O & icky stuff	CO_2 & H_2O	H_2O
Manufacturable on Mars?	No	Yes	Yes

Figure 1.1: Comparison of different fuel

Now, looking at the oxidizer-fuel ratios (expressed in mass unit), we see that RP-1 is burned at 2.7 grams of oxygen to 1 gram of RP-1, Hydrogen burns at 6 grams of oxygen to 1 grams of hydrogen, and Methane burns at 3.7 grams oxygen to 1 grams Methane. These numbers can help offset a little the massive difference in density.
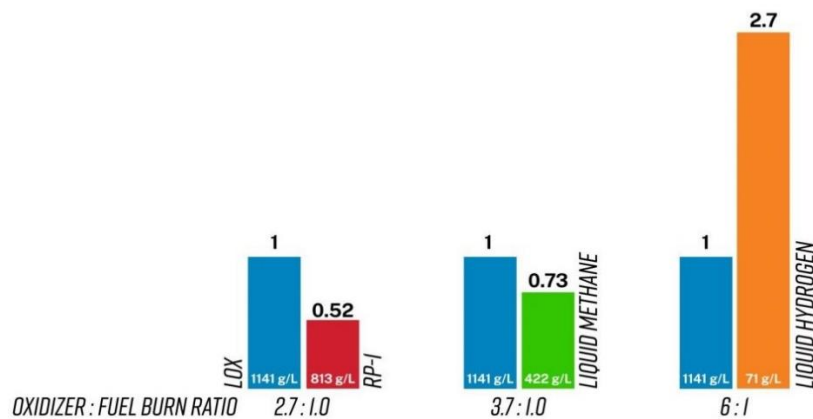
Figure 1.2: OF burn ratio comparison

This graph can help us to have an idea about the ratios. The density of liquid oxygen is 1,141 grams per liter, so a little denser than RP-1 which density is (as we can see) 813 grams per liter. So, burning LOX and RP-1 at a 2.7 to 1 ratio, for every liter of LOX you'd need a little over half a liter of RP-1. Then we analyze Hydrogen which is 11 times less dense than RP-1. Luckly a 6:1 burning ratio is

perfect for Hydrogen and this ratio can help to avoid a tank 11 times bigger than the one for the RP-1, using instead one 5 times bigger, burning 2.7 liters of Hydrogen for each liter of LOX.

Looking at the methane, LOX is 2.7 times more dense than liquid methane, but the burn ratio is 3.7 grams of oxygen to 1 gram of methane. So, you'd need 0.73 liters of methane for every liter of LOX. This means that the fuel tank would need to be 40% bigger for methalox than it would need to be for RP-1, despite RP-1 being almost twice as dense. Compared to Hydrogen, it's fuel tank would be 3.7 times smaller. The fuel to oxidizer ratio helps make Methalox's fuel tanks a lot closer to RP-1 than it is to Hydrolox in terms of space needed.

Next up is the efficiency measured in terms of specific impulse because the higher the specific impulse, the less fuel it takes to do the same amount of work. Due to the molecular weight of each fuel and their energy released when burned, there's a different potential for how quickly the exhaust gas can be expelled out the nozzle. Ideally an RP-1 powered engine could achieve about 370 seconds, an ideal Hydrogen powered engine could get 532 seconds and a methane powered engine is in the middle with 459 seconds. The real world has given us some examples which the maximum values are lower than expected: RP-1 engines seeing around 350 seconds (with Merlin 1D Vacuum), around 380 seconds for a methane engine (with Raptor vacuum) and about 465 seconds for a hydrogen engine (with RL-10B-2).

After that we have the combustion point, a temperature which indicates how hot each fuel burns. A fuel that burns cooler is easier on the engine and potentially makes for a longer lifespan. RP1 can burn up to 3670 K, Hydrogen 3070 K and, as we can see for every other parameter, Methane is again between the two at 3550 K.

Then we see that RP-1 has a very high boiling point, even higher than water at 490 K. Hydrogen on the other hand is near absolute zero at an incredibly cold 20K. This takes serious considerations to keep anything at that temperature. Methane is between the two at 111 K, cold and requires thermal considerations, but it boils off at a temperature like LOX. And because of this similarity in terms of boiling point, the tanks can share a common dome, which makes the vehicle lighter.

At last, we must consider that SpaceX's ultimate goals are to develop a system capable of taking humans out to Mars and back over and over, so using a fuel that can be made using Mars' resources could be good economically and also in terms of weight of the vehicle. Methane could be produced on Mars using the Sabatier process. This reaction combines hydrogen and carbon dioxide ($CO_2 + 4H_2 \rightarrow CH_4 + 2H_2O$) to create water and methane. Initially, water extracted from Mars' poles would be broken down into hydrogen through water electrolysis. Subsequently, the hydrogen and carbon dioxide would be mixed and heated at a high temperature with the help of a nickel catalyst, resulting in the formation of methane and water vapor. This procedure can be repeated using the generated water, establishing a cyclic process that produces oxygen and fuel from carbon dioxide.

At the end we can say that methane is the right choice for SpaceX because it's fairly dense meaning the rockets size remains reasonable, it's fairly efficient, it burns clean and makes for a highly reusable engine, it burns relatively cool helping expand the lifespan of an engine, which again is good for reusability, it's cheap and easy to produce and can be easily produced on the surface of Mars.

2 Symbology

Table 2.1: Symbology

$\dot{m}_p$	Propellant Mass Flow	$\frac{kg}{s}$	D_c	Combustion Chamber Section Diameter	m
$\dot{m}_f$	Fuel Mass Flow	$\frac{kg}{s}$	Γ	Nozzle Area Ratio Parameter	-
$\dot{m}_{ox}$	Oxidizer Mass Flow	$\frac{kg}{s}$	γ	Specific Heat Ratio of Exhaust Gas	-
o/f	Mixture Ratio	-	A_t	Throat Section Area	m^2
$I_{sp,id}$	Ideal Specific Impulse	s	D_t	Throat Section Diameter	m
I_{sp}	Real Specific Impulse	s	A_e	Exit Section Area	m^2
$c_{t,id}$	Ideal Thrust Coefficient	-	ε	Nozzle Area Ratio	-
c_t	Real Thrust Coefficient	-	D_e	Exit Section Diameter	m
$u_{e,id}$	Ideal Flux Velocity at the Nozzle Exit Plane	$\frac{m}{s}$	P_e	Exit Section Pressure	bar
u_e	Real Flux Velocity at the Nozzle Exit Plane	$\frac{m}{s}$	T_{ex}	Exit Section Temperature	K
η	Efficiency Coefficient	-	V_c	Combustion Chamber Volume	m^3
ρ_c	Combustion Chamber Density	$\frac{kg}{m^3}$	L^*	Characteristic Length of the Combustion Chamber	m
P_c	Combustion Chamber Pressure	bar	L_{cyl}	Length of the Combustion Chamber	m
T_c	Combustion Chamber Temperature	K	L_c	Convergent Length	m
M_M	Molecular Mass of the Exhaust Gas	$\frac{g}{mol}$	α_{conv}	Convergent Angle	deg
R	Specific Exhaust Gas Constant	$\frac{J}{kg \cdot K}$	L_e	Divergent Lenght	m
A_c	Combustion Chamber Section Area	m^2	α_{div}	Divergent Angle	deg
u_c	Flux Velocity at the Exit of the Combustion Chamber	$\frac{m}{s}$	z_{opt}	Optimal Altitude	m

T_{std}	Standard Temperature	K	η_{pump}	Adiabatic Efficiency of the Pump	-
P_{std}	Standard Pressure	Pa	ΔP	Generic Pressure Loss	bar
T_{sl}	Sea Level Thrust	N	T_{tankOX}	Oxygen Tank Temperature	K
b	Convergent Angle	deg	T_{tankF}	Fuel Tank Temperature	K
R_1	First Near Throat Connection Radius	m	P_{tankOX}	Oxygen Tank Pressure	bar
R_t	Throat Section Radius	m	P_{tankF}	Fuel Tank Pressure	bar
R_2	Near Comb. Chamber Connection Radius	m	ρ_{LOX}	Liquid Oxygen Density	$\frac{kg}{m^3}$
R_n	Second Near Throat Connection Radius	m	ρ_{LCH4}	Liquid Fuel Density	$\frac{kg}{m^3}$
T	Generic Thrust	N	K_s	Safety Factor for Tank Dimensioning	-
T_n	Starting Divergent Angle	deg	t_b	Burning Time	s
T_e	Exit Divergent Angle	deg	M_{LCH4}	Liquid Fuel Mass	kg
c_p	Specific Heat at Constant Pressure	$\frac{J}{kg \cdot K}$	M_{LOX}	Liquid Oxygen Mass	kg
h_x	Real Enthalpy	$\frac{J}{kg}$	V_{LCH4}	Liquid Fuel Volume	m^3
h'_x	Ideal Enthalpy	$\frac{J}{kg}$	V_{LOX}	Liquid Oxygen Volume	m^3
η_s	Isentropic Coefficient	-	γ_{He}	Helium Specific Heat Ratio	-
P_{pump}	Pump Pressure	bar	R_{He}	Helium Specific Constant	$\frac{J}{kg \cdot K}$
Δh_{pump}	Enthalpy Difference for the Pump	$\frac{J}{kg}$	T_{He_i}	Starting Helium Temperature	K
Δh_{turb}	Enthalpy Difference for the Turbine	$\frac{J}{kg}$	ρ_{AV}	Weighted Average Density	$\frac{kg}{m^3}$
η_{mecc}	Mechanical Efficiency of the Turbine	-	I_v	Volumetric Impulse	$\frac{kg \cdot s}{m^3}$
η_{turb}	Adiabatic Efficiency of the Turbine	-	I_{tot}	Total Impulse	$N \cdot s$

P_{He_i}	Starting Helium Pressure	bar
M_{He}	Helium Mass	kg
V_{He}	Helium Volume	m^3
$NPSH$	Net Positive Suction Head	m
T_{out}	Outlet Temperature of the Cooling System	K

R	Gas Constant	$\dfrac{J}{mol \cdot K}$
D_{1H}	One Hole Injector Diameter	m
ρ_F	Fuel Rich Density	$\dfrac{kg}{m^3}$
ρ_{OX}	Oxidizer Rich Density	$\dfrac{kg}{m^3}$

3 Thrust Chamber

The sizing of the engine was made using NASA-CEA's rocket problem and entering the following parameters:

- Pressure in the combustion chamber
- Mixture ratio
- Nozzle area ratio

It may seem illogical to enter the nozzle area ratio as initial parameter as it should be obtained at the end of the calculations, but it proves to be much more accurate. Indeed, if we were to use the normal procedure of calculating first the velocity at the nozzle exit plane and then the nozzle area ratio, we would find an exit temperature much higher than the real one. That is because with:

$$v_c = \sqrt{\frac{T \cdot R}{M} \cdot \frac{2 \cdot \gamma}{\gamma - 1}\left[1 - \left(\frac{P_e}{P}\right)^{\frac{\gamma-1}{\gamma}}\right]}$$

$$\frac{A_2}{A^*} = \frac{1}{\mathcal{M}_2}\left[\frac{2}{\gamma+1}\left(1 + \frac{\gamma-1}{2}\mathcal{M}_2\right)\right]^{\frac{\gamma+1}{2(\gamma-1)}}$$

we assume the γ to be constant throughout the nozzle length, instead during the combustion the γ increases by 10%. Thus, we must use the CEA to determine the performance parameters and physical properties of the exhaust gas such as pressure and temperature in the several parts of the nozzle.

The software Nasa CEA offers two different methods to study the isentropic expansion that happens during the combustion: shifting equilibrium and frozen equilibrium, the first implies that the exhaust gas changes its chemical composition to match the local expanding conditions in the nozzle, while the second method fixes the chemical mixture of the exhaust gas.

The best approximation assumes shifting equilibrium from the combustion chamber to the nozzle throat and frozen equilibrium from the throat to the exhaust.

The initial parameters of the engine (pressure in the combustion chamber, mixture ratio, nozzle area ratio and propellant mass flow) used in the calculations were taken from a report made by the German Aerospace Center which was considered a trustworthy source.

3.1. Calculations

First, considering the propellant mass flow and the mixture ratio, the mass flow of fuel and oxidizer are found as:

$$\dot{m}_f = \frac{\dot{m}_p}{o/f + 1}$$

$$\dot{m}_{ox} = \dot{m}_p - \dot{m}_f$$

Afterwards, the ideal specific impulse, coefficient of thrust and the velocity at the nozzle exit plane, obtained through CEA, are slightly lowered as they are multiplied by an efficiency coefficient η that gives the real values.

$$I_{sp} = I_{sp,id} * \eta$$

$$c_t = c_{t,id} * \eta$$

$$u_e = u_{e,id} * \eta$$

Next, the density of the exhaust gas and the diameter of the combustion chamber are determined.

$$\rho_c = \frac{P_c*10^5}{T_c*R}$$

$$A_c = \frac{\dot{m}_p}{\rho_c*u_c}$$

$$D_c = \sqrt{\frac{4*A_c}{\pi}}$$

The diameter of the throat is found using the Vandenkerckhove function that allows to calculate Γ used throughout the calculations.

$$\Gamma(\gamma) = \sqrt{\gamma * \left(\frac{1}{\gamma+1}\right)^{\frac{\gamma+1}{\gamma-1}}}$$

$$A_t = \frac{\dot{m}_p\sqrt{T_c*R}}{\Gamma*P_c*10^5}$$

$$D_t = \sqrt{\frac{4*A_t}{\pi}}$$

The diameter at the exit is found by knowing the diameter of the throat and the nozzle ratio ε. Finally, the length of the combustion chamber is found. (Using L*=1.3m)

$$A_e = A_t * \varepsilon$$

$$D_e = \sqrt{\frac{4*A_e}{\pi}}$$

$$V_c = A_t L^*$$

$$L_{cyl} = \frac{V_c}{A_c}$$

To determine the dimensions of the nozzle, the code first fixes the angle of the convergent part of the nozzle to 15 degrees and then fixes the divergent part of the nozzle to 45 degrees. However, in real life, nozzles have a bell shape. A more accurate analysis on the performance of different type of nozzles will be discussed in the next chapter.

$$L_c = \frac{1}{2} \frac{(D_c - D_t)}{tan(\alpha_{conv})}$$

$$L_e = \frac{1}{2} \frac{(D_e - D_t)}{tan(\alpha_{div})}$$

To determine the optimal altitude the ideal velocity at the nozzle exit plane is used. The reason is that, as stated before, to determine the exit pressure from the real velocity at the nozzle exit plane one must use formulas with constant γ which inevitably makes it inaccurate.

$$z_{opt} = \frac{T_{std}}{\alpha} \cdot \left(1 - \frac{P_e \cdot 10^5}{P_{std}}\right)^{\frac{R \cdot \alpha}{g}}$$

At last, we determined the Sea level Thrust that the engine should have with the given mass propellent flow with the equation ($Pstd = 101325 \cdot 10^5$):

$$Tsl = \dot{m}p \cdot ue + (Pe \cdot 10^5 - Pstd) \cdot Ae$$

3.2. Performance Parameters R1's and R2's comparison

The sizing of Raptor 2 was made using the same formulas used for sizing Raptor 1. The main differences between the two versions of the raptors are: the pressure in the combustion chamber and the different propellent mass flows that go through the engine. The pressure increases by 20% going from 250 bar to 300 bar (Figure 3.5) while the propellent mass flows increases by 28 % going from 530 kg/s to 681 kg/s (Figure 3.1). This enables the engine to deliver a remarkable increase of 30% Sea-level thrust as can be seen in Figure 3.4 The optimal altitude also varies significantly almost halving its height in its second version (Figure 3.6). On the other hand, engine parameters have only slight variations. The Thrust coefficient changes by only 0.002 and the length of the combustion chamber by only 0.0003 m (Figure 3.2, Figure 3.3). Engine dimensions change but not by large margins: the throat section diameter changes by 4.1% allowing higher mass flows.

Table 3.1: CEA Input

	Raptor 1 engine	Raptor 2 engine
P_c	250	300
o/f	3.6	3.4
ε	35	34.34

Table 3.2: CEA Results

	Raptor 1 engine	Raptor 2 engine
T_c	3737.6	3741.6
P_e	0.59323	0.72628
T_{ex}	1384.8	1381.8
M_M	22.853	22.338
γ	1.2339	1.2356

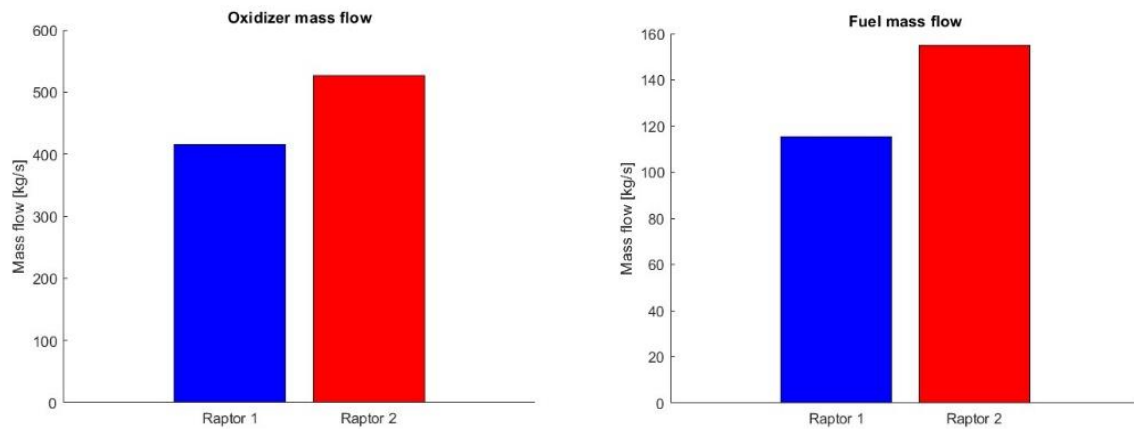|		
R	363.80	372.19
u_e	3217.6	3247.2
$\dot{m}_{ox}$	415.17	526.91
$\dot{m}_f$	115.32	154.97
I_{sp}	328.01	331.02
c_t	1.7416	1.7395
T_{sl}	1651.4	2173.9
z_{opt}	4915.2	2998.2
D_c	0.35674	0.37120
L_{cyl}	0.49132	0.49166
D_t	0.21931	0.22828
D_e	1.2974	1.3377
L_c	0.068713	0.071459
L_e	2.0118	2.0702

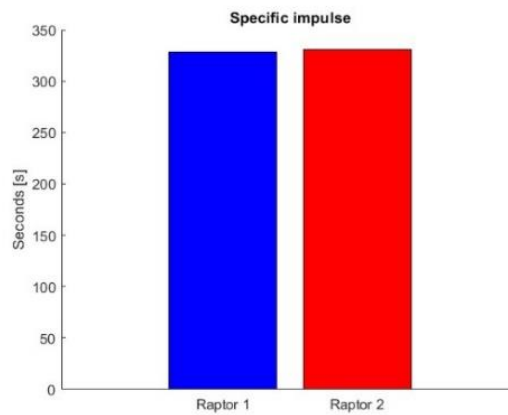Figure 3.1: Raptor 1 and Raptor 2 oxidizer and fuel mass flow

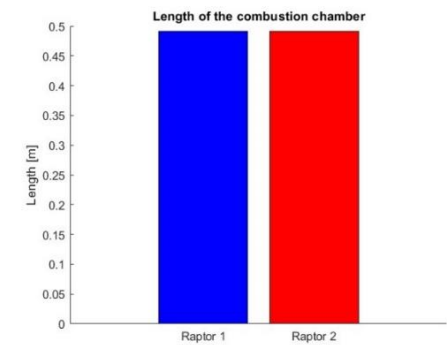Figure 3.2: Raptor 1 and Raptor 2 specific impulse

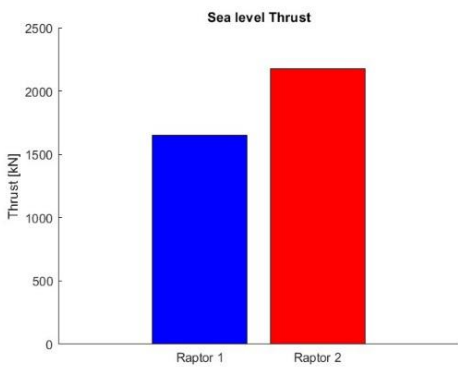Figure 3.3: Raptor 1 and Raptor 2 combustion chamber length

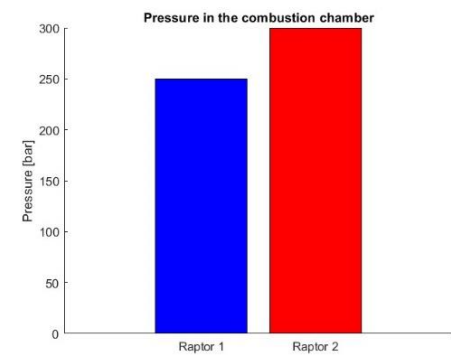Figure 3.4: Raptor 1 and Raptor 2 sea level thrust

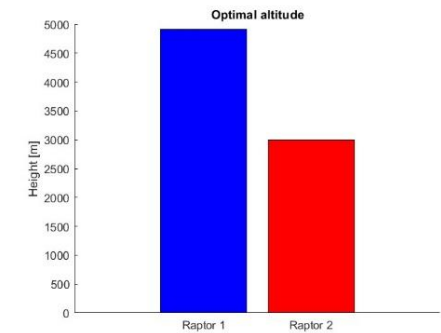Figure 3.5: Raptor 1 and Raptor 2 combustion chamber pressure

Figure 3.6: Raptor 1 and Raptor 2 optimal altitude

4   RPA Analysis

4.1.   Introduction

RPA, which stands for Rocket Propulsion Analysis, is an analysis tool for conceptual and preliminary design of chemical rocket engines, widely used in the space industry for the design, analysis and optimization of space rocket engines. It utilizes various mathematical principles to run its calculations and simulations. In particular, it employs the fundamental principles of fluid dynamics, thermodynamics and combustion theory to compute and analyse the flow of gases within the rocket engine, allowing the users to have a preliminary sizing of the engine, while also predicting some important performance parameters. RPA calculates critical parameters such as specific impulse, thrust in vacuum and at sea level, thrust coefficient and nozzle dimensions by using data inputs given by the users. These inputs are: propellant properties, chamber pressure, combustion chamber geometry, nozzle design requirements and operating conditions. RPA allows the study of all types of rocket engines, such as solid, liquid and hybrid propulsion systems. In this study, the software has been utilized to realize the preliminary design and performance simulations of the Raptor 1 and Raptor 2 engines, analysing both conical and bell nozzles to see the difference in size, performance and geometry design. The software also gives the possibility to export the contours of the engine, which has then been used to make a 3D model of the different designs using Dassault Systèmes Solidworks. These designs were later utilized to run simulations of the fluid flow and heat transfer inside the engines using Ansys and its CFD module Fluent, which will be discussed in the next chapter of this report. In the next section, the results will be presented for the different geometries, comparing parameters.
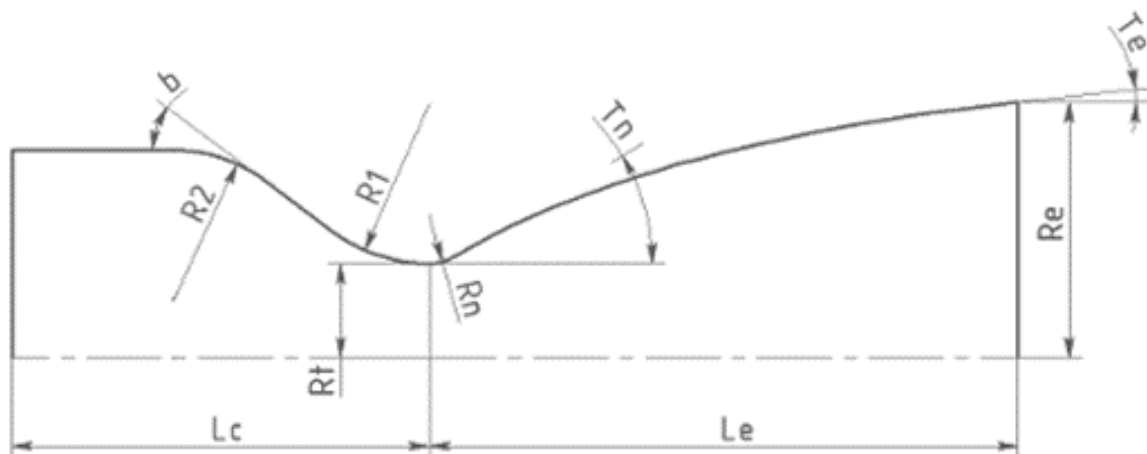

Figure 4.1: Nozzle 3D Model

4.2.   Raptor 1

The RPA software has been used to size the Raptor 1 engines using the following data as input:
- Engine definition:
  - $P_c = 250$ bar
  - $\dot{m}_p = 530.5\ kg/s$
- Propellant specification:
  - System bipropellant
  - $o/f = 3.6$
  - Oxidizer Liquid Oxygen (LOX)
  - Fuel: Liquid Methane (LCH4)
- Nozzle flow model:
  - $\varepsilon = \frac{A_e}{A_t} = 35$
  - $P_{std} = 101325\ Pa$
- Engine design parameters:
  - $L^* = 1.30$ m
  - $b = 30$ deg
  - $\frac{R_1}{R_t} = 1.5$
  - $\frac{R_2}{R_{2\,Max}} = 0.500$
  - $\frac{R_n}{R_t} = 0.382$

As for the nozzle shape, the study was done for both conical and bell nozzle and will be now discussed separately. It is also important to note that the reaction efficiency of the engine was not predefined by the user, but it was estimated by the software on the basis of defined engine parameters.

4.2.1.   Cone Nozzle

In the first case, the nozzle shape was set as a conical nozzle with 15 degrees half angle. The analysis gave the following results.

Table 4.1: Raptor 1 Cone Nozzle Thrust and Mass Flow Rates

Symbol	Value
$T\ (vac)$	1838.8812 kN
$I_{sp}(vac)$	353.4660 s
$T\ (opt)$	1732.1521 kN
$I_{sp}(opt)$	332.9507 s
$\dot{m}_p$	530.5000 $\frac{kg}{s}$
$\dot{m}_{ox}$	415.1739 $\frac{kg}{s}$
$\dot{m}_f$	115.3261 $\frac{kg}{s}$

Table 4.2: Raptor 1 Cone Nozzle Geometry

Symbol	Value	Symbol	Value
D_c	330.81 mm	L_{cyl}	496.77 mm
b	30.00 deg	D_t	227.09 mm
R_2	108.39 mm	R_n	43.37 mm
R_1	170.32 mm	L_e	2088.93 mm
L^*	1300.00 mm	T_e	15.00 deg
L_c	661.27 mm	D_e	1343.49 mm
Divergence efficiency: 0.9830			

Exporting the engine contour, it was also possible to have a visual representation of the engine and its size:
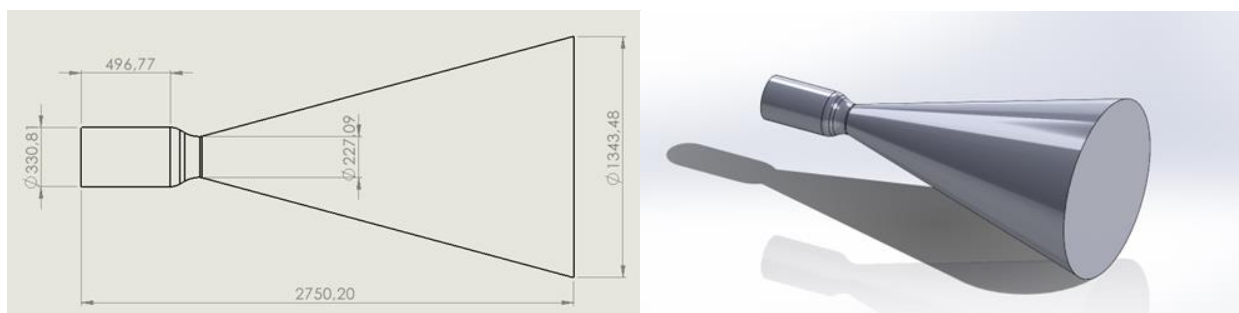

Figure 4.2: Cone Nozzle Raptor 1

4.2.2. Bell Nozzle

In the second case the nozzle shape was set as a bell nozzle with efficiency estimated for length 80% on the basis of the defined exit conditions. The analysis gave the following result.

Table 4.3: Raptor 1 Bell Nozzle Thrust and Mass Flow Rates

Symbol	Value
$T\,(vac)$	1848.7761 kN
$I_{sp}(vac)$	355.36794 s
$T\,(opt)$	1742.0469 kN
$I_{sp}(opt)$	334.8527 s
$\dot{m}_p$	530.5000 $\frac{kg}{s}$
$\dot{m}_{ox}$	415.1739 $\frac{kg}{s}$
$\dot{m}_f$	115.3261 $\frac{kg}{s}$

Table 4.4: Raptor 1 Bell Nozzle Geometry

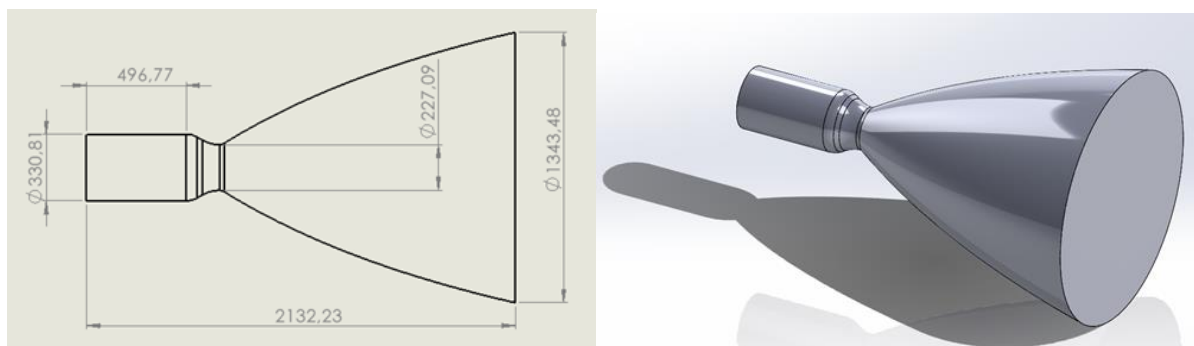| Symbol	Value	Symbol	Value
D_c	330.81 mm	D_t	227.09 mm
b	30.00 deg	R_n	43.37 mm
R_2	108.39 mm	T_n	31.80 deg
R_1	170.32 mm	L_e	1470.96 mm
L^*	1300.00 mm	T_e	12.78 deg
L_c	661.27 mm	D_e	1343.49 mm
L_{cyl}	496.77 mm	$\frac{L_e}{D_t}$	6.48
Divergence efficiency: 0.9826			
Drag efficiency: 0.9636			

Figure 4.3: Bell Nozzle Raptor 1

4.2.3. Comparison between C – D, conical, and bell nozzles

Here are the different characteristic dimensions of the engine for the different nozzle geometries:

Table 4.5: Different nozzle geometries for Raptor 1

[mm]	C − D Nozzle	Cone Nozzle	Bell Nozzle
D_c	356.74	330.81	330.81
D_t	219.31	227.09	227.09
D_e	1297.46	1343.49	1343.49
L_{cyl}	491.32	496.77	496.77
L_c	687.13	661.27	661.27
L_e	2011.86	2088.93	1470.96

As we can see, the conical and parabolic nozzle computed using the RPA software have the same dimensions, except the length of the divergent segment, which is significantly shorter for the bell nozzle, due to its parabolic shape.

The C-D nozzle calculated with the procedure displayed in the previous chapters has a wider chamber (+7.8% on the diameter of the chamber) and tighter throat end exit sections (-3.42% on throat and exit diameters). The length of the C-D nozzle is similar to the conical nozzle, with a significantly longer divergent segment compared to the bell nozzle for the same reasons discussed above.

As for the two main performance parameters, the differences between the three possible engines are now showcased:

Table 4.6: Main performance parameters for different nozzle geometries for Raptor 1

	C − D Nozzle	Cone Nozzle	Bell Nozzle
T_{sl}[1] [kN]	1651.43	1702.64	1711.77
I_{sp} (sea level) [s]	328.02	327.28	329.03

We can see that the most performing engine is the one with the parabolic nozzle, improving the thrust at sea level by 3.65% compared to the C-D nozzle and by 0.54% compared to the Cone Nozzle and the specific impulse by 0.307% from the C-D nozzle and by 0.535% from the Cone Nozzle.

4.3. Raptor 2

The RPA software computed the analysis to size the Raptor 2 engine with the following data as input:

- Engine definition:
  - $P_c = 300$ bar
  - $\dot{m}_p = 681.89\ kg/s$

---

[1] Thrust and Specific Impulse were calculated multiplying the ideal values taken from the RPA software by the divergence efficiency.

- Propellant specification:
    - System bipropellant
    - $o/f = 3.4$
    - Oxidizer Liquid Oxygen (LOX)
    - Fuel: Liquid Methane (LCH4)
- Nozzle flow model:
    - $\varepsilon = \frac{A_e}{A_t} = 34.34$
    - $P_{std} = 101325\ Pa$
- Engine design parameters:
    - $L^* = 1.30\ \text{m}$
    - $b = 30\ \text{deg}$
    - $\frac{R_1}{R_t} = 1.5$
    - $\frac{R_2}{R_{2_{MAX}}} = 0.500$
    - $\frac{R_n}{R_t} = 0.382$

As for the nozzle shape, the study was done only for the bell nozzle, since the previous analysis for the Raptor 1 highlighted that this is the most performing geometry. In this study the reaction efficiency of the engine was also not predefined by the user, but it was estimated by the software on the basis of defined engine parameters.

4.3.1. Bell Nozzle

The nozzle shape was set as a bell nozzle with efficiency estimated for length 80% based on the defined exit conditions. The analysis gave the following results:

Table 4.7: Raptor 2 Bell Nozzle Thrust and Mass Flow Rates

Symbol	Value
$T\ (vac)$	2383.85422 kN
$I_{sp}(vac)$	356.48782 s
$T\ (opt)$	2254.62929 kN
$I_{sp}(opt)$	337.16318 s
$\dot{m}_p$	681.89 $\frac{kg}{s}$
$\dot{m}_{ox}$	526.915 $\frac{kg}{s}$
$\dot{m}_f$	154.975 $\frac{kg}{s}$

Table 4.8: Raptor 2 Bell Nozzle Geometry

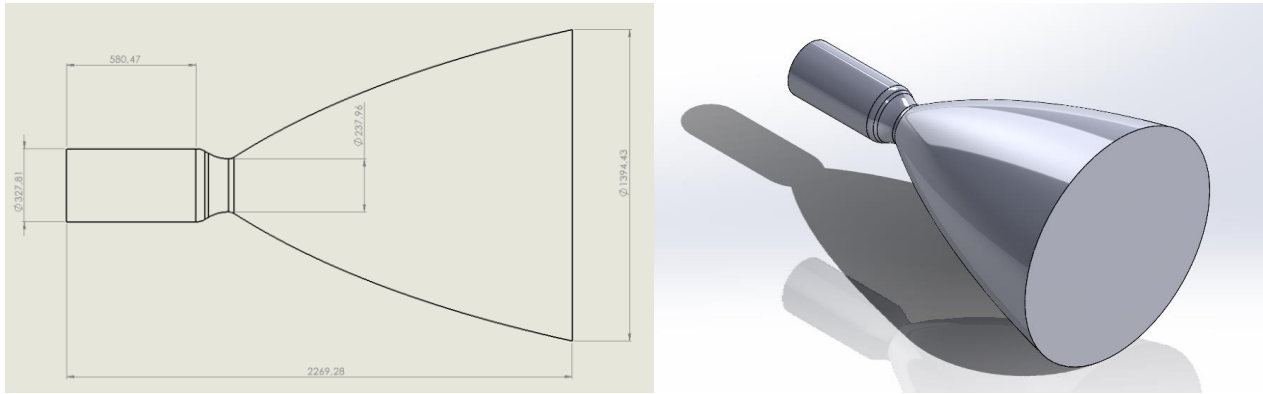| Symbol	Value	Symbol	Value
D_c	327.81 mm	D_t	237.95 mm
b	30.00 deg	R_n	45.45 mm
R_2	78.44 mm	T_n	32.42 deg
R_1	178.47 mm	L_e	1542.15 mm
L^*	1300.00 mm	T_e	12.29 deg
L_c	727.12 mm	D_e	1343.49 mm
L_{cyl}	580.47 mm	$\frac{L_e}{D_t}$	6.48
Divergence efficiency: 0.9832			
Drag efficiency: 0.9633			

Figure 4.4: Bell Nozzle Raptor 2

4.3.2. Comparison between C – D and bell nozzles

Here are the different characteristic dimensions of the engine for the two different nozzle geometries:

Table 4.9: Different nozzle geometries for Raptor 2

[mm]	C − D Nozzle	Bell Nozzle
D_c	371.20	327.81
D_t	228.28	237.95
D_e	1337.73	1343.49
L_{cyl}	491.66	580.47
L_c	714.59	727.12
L_e	2070.27	1542.15

As we can see, the C-D nozzle calculated in the previous chapters has a wider chamber (+13.24% on the diameter) and tighter throat end exit sections (-4.06% on the diameters), as it was the case for the Raptor 1.

The length of the C-D nozzle is shorter in the segment of the chamber and the convergent section, but it has a significantly longer divergent segment compared to the bell nozzle.

As for the two main performance parameters, we can look at the differences between the two engines:

Table 4.10: Main performance parameters for different nozzle geometries for Raptor 2

	C − D Nozzle	Bell Nozzle
T_{sl}[2] [kN]	2173.85	2216.80
I_{sp} (sea level) [s]	331.02	331.51

We can see that the engine that has better performance is the one with the parabolic nozzle, improving the thrust at sea level by 1.98% and the specific impulse by 0.148% compared to the C-D nozzle.

---

[2] Thrust and Specific Impulse were calculated multiplying the ideal values taken from the RPA software by the divergence efficiency.

5   ANSYS Analysis

5.1.   Introduction

Ansys is a software tool utilized to run simulations and analysis of fluid flow and heat transfer in complex systems with its CFD module, Fluent. Ansys employs mathematical principles as well as numerical methods to compute various physical phenomena, leveraging techniques from the finite element analysis (FEA) field, computational fluid dynamics (CFD) and other disciplines to predict and analyse the behaviour of structures, fluids and heat transfer.

Using the Navier-Stokes equations, which describe the motion of fluids, and integrating them with turbulence models it analyses the behaviour of fluid flow and its interactions with solid surfaces.

For didactic reasons, having never dealt with a CFD software before, simplifications were made in order to carry out the analysis, assuming an ideal gas with constant properties within the engine. This simplifying assumption led to less accurate results, but still provided important information about the operation and behaviour of various parameters such as pressure, temperature, and velocity inside the analysed engines.

In the following paragraphs, the results will be presented for the different geometries of both Raptor 1 and 2 engines, with a final comparison of performances to see which design is the most efficient and accurate to the mission purposes.

5.2.   Raptor 1

5.2.1.   Geometry and Mesh

After creating and importing the 3D models of the three different engines, they were imported in Ansys to compute the analysis of their functioning.

Before the calculations, the meshing process needs to be done: this process divides the geometry into a collection of smaller, interconnected, finite elements, such as tetrahedra or hexahedra in 3D. For this solution, the method used was the automated meshing process of Ansys.
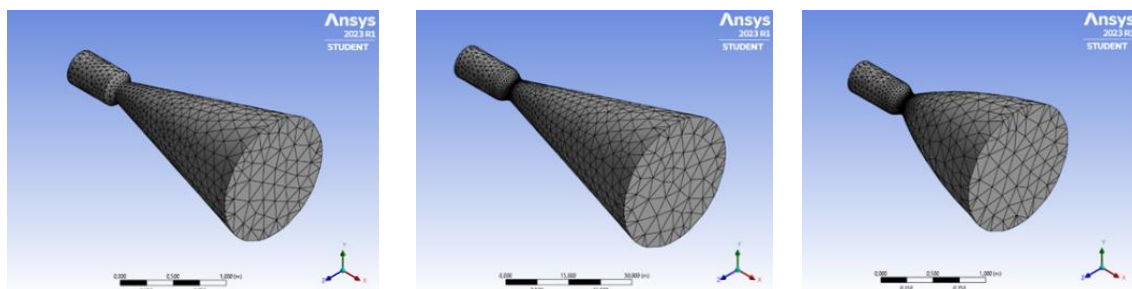

Figure 5.1: Raptor 1 C – D, Cone, and Bell Nozzle Geometry

5.2.2. Fluent Settings

After having discretized the models, the solution can be run using Ansys' CFD module, Fluent.

In this software the settings of the model were to have the Energy model turned on and the fluid was considered inviscid.

As for the liquid flow, a simplification was made to consider the flow as an ideal gas with constant specific heat and molar mass. These parameters were taken from the CEA output from the properties at the beginning and were considered static throughout the whole process ($c_p = 2302.5 \frac{J}{kg \cdot K}$, $M_M = 22.573 \frac{g}{mol}$). This simplified approach led to imperfect results, even if they still provided some interesting information about the different performances of the engines.

Given the boundary conditions of pressure and temperature at the inlet and the outlet of the system, it was possible to initialize the solution computing from the inlet.

Once the initialization was done, it was possible to compute the solution for the three engines.

5.2.3. Results and Comparison

Thanks to the solution obtained, the contour of some physical quantities of interest can be displayed, such as velocity magnitude (and Mach number), static temperature and static pressure.

Velocity magnitude and Mach number

In the following contours we can see the progress of the flow velocity and Mach number for the different engines:

- C-D Nozzle:
    - Maximum velocity magnitude (outlet): 3251.143 m/s
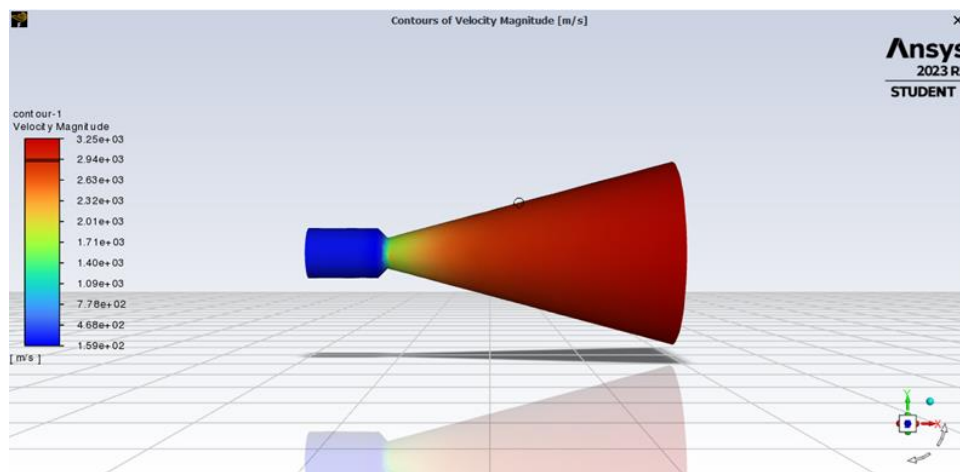   - Maximum Mach number (outlet): 4.088

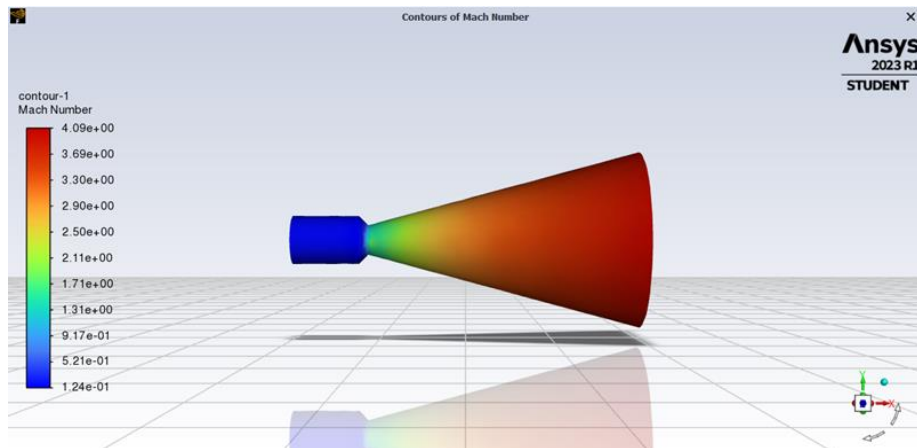Figure 5.2: Raptor 1 C – D Nozzle Maximum Velocity Magnitude

Figure 5.3: Raptor 1 C – D Nozzle Maximum Mach Number

- Cone nozzle:
    o Maximum velocity magnitude (outlet): 3259.362 m/s
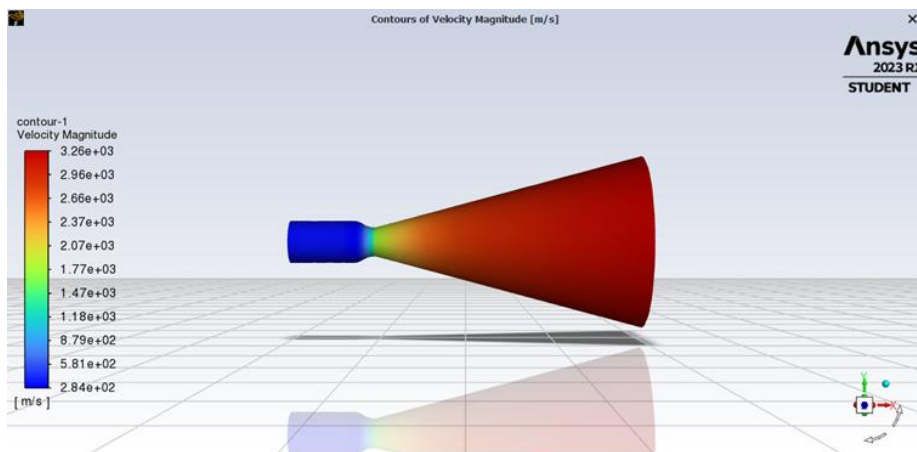   o Maximum Mach number (outlet): 4.115

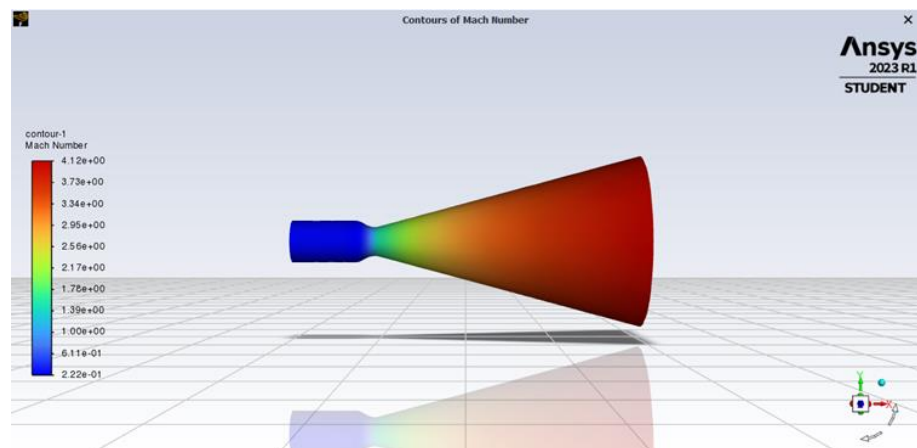Figure 5.4: Raptor 1 Cone Nozzle Maximum Velocity Magnitude

Figure 5.5: Raptor 1 Cone Nozzle Maximum Mach Number

- Bell Nozzle:
  - Maximum velocity magnitude (outlet): 3298.65 m/s
  - Maximum Mach number (outlet): 4.249

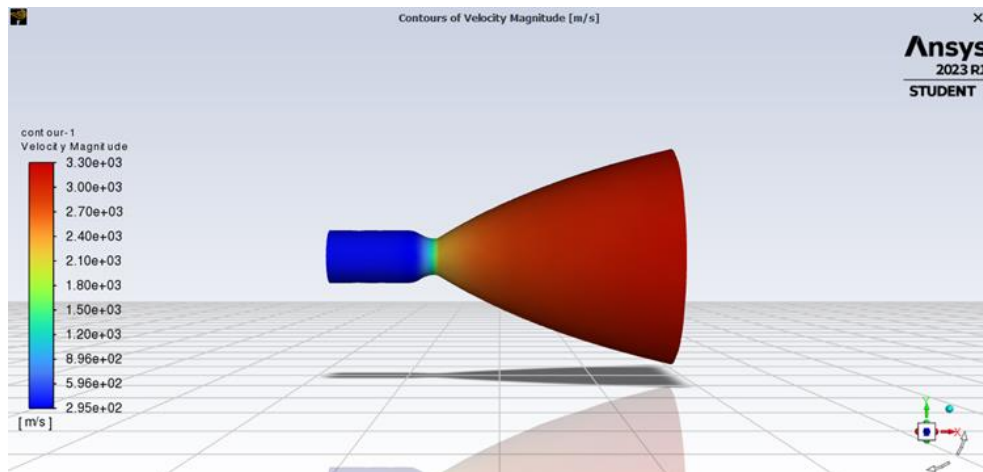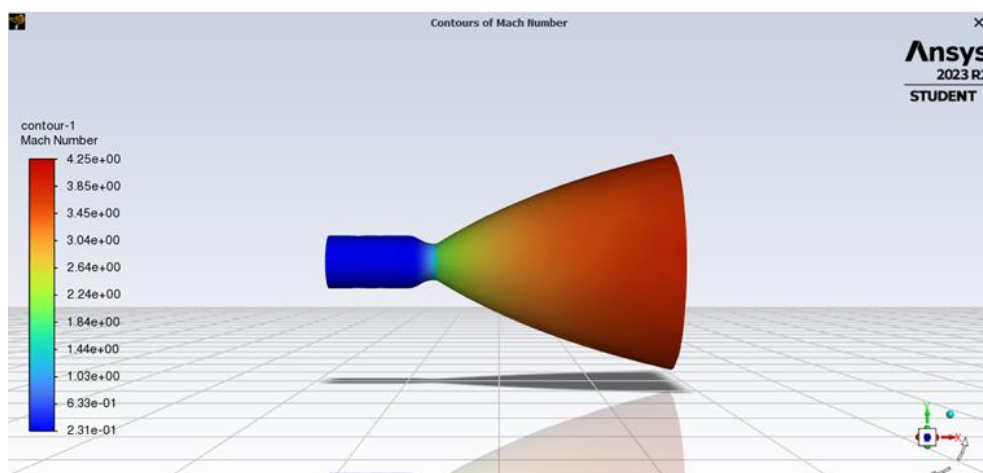Figure 5.6: Raptor 1 Bell Nozzle Maximum Velocity Magnitude

Figure 5.7: Raptor 1 Bell Nozzle Maximum Mach Number

As we can see, the bell nozzle is the most efficient engine when it comes to the velocity magnitude at the exit, improving from the C-D and Cone Nozzle by +1.46% and +1.21%.

Static Temperature

Here are the graphics of the progress of static temperature in the three engines along the X axis of the motor.

- C-D Nozzle:
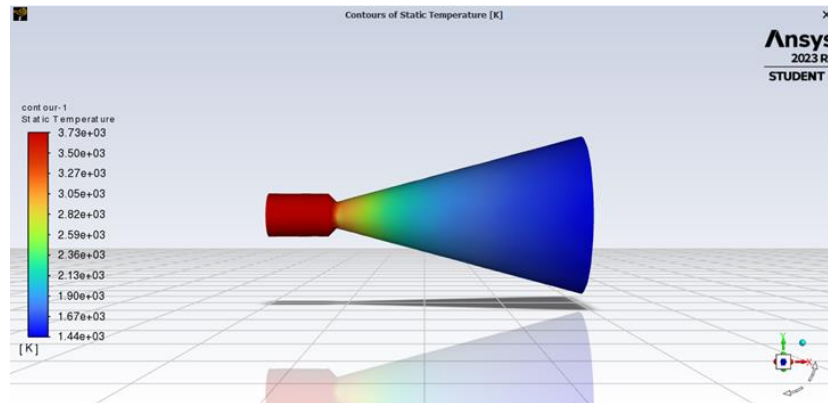 - o Minimum static temperature (outlet): 1442.278 K

Figure 5.8: Raptor 1 C – D Nozzle Minimum Static Temperature

- Cone Nozzle:
  - o Minimum static temperature (outlet): 1430.675 K
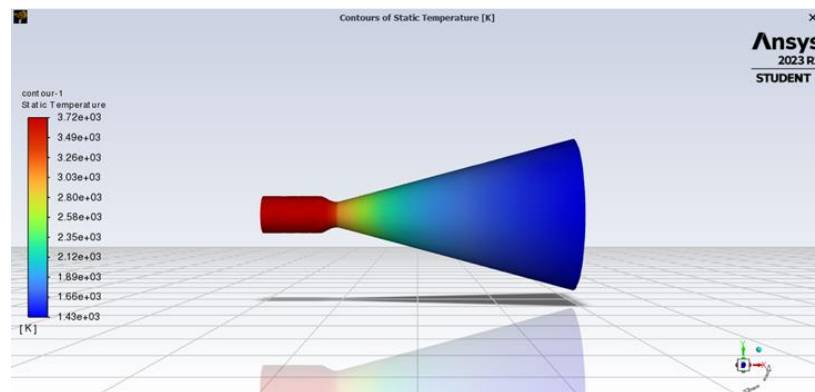
Figure 5.9: Raptor 1 Cone Nozzle Minimum Static Temperature

- Bell Nozzle:
  - o Minimum static temperature (outlet): 1374.719 K
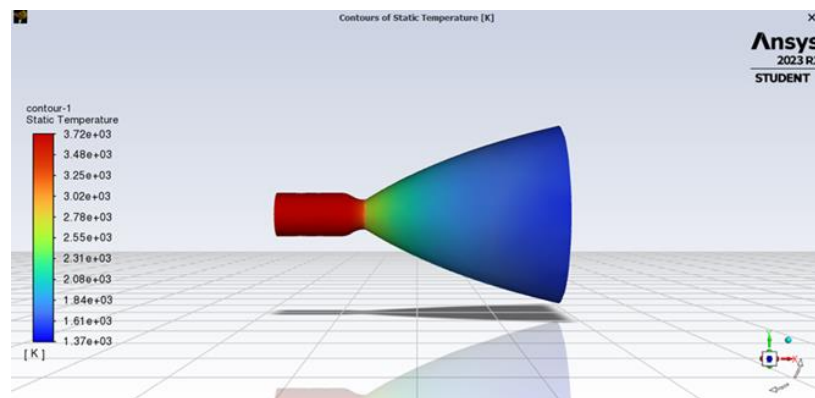
Figure 5.10: Raptor 1 Bell Nozzle Minimum Static Temperature

For this parameter, the bell nozzle proves to be the one reaching the overall minimum static temperature of the three engines, lowering it by -6.56 % from the C-D Nozzle case and by -5.80 % from the Cone Nozzle.

<u>Static Pressure</u>

Here are the contours for the progress of static pressure in the three engines.

- C-D Nozzle:
  - o Minimum static gauge pressure (outlet): -42699.03 Pa
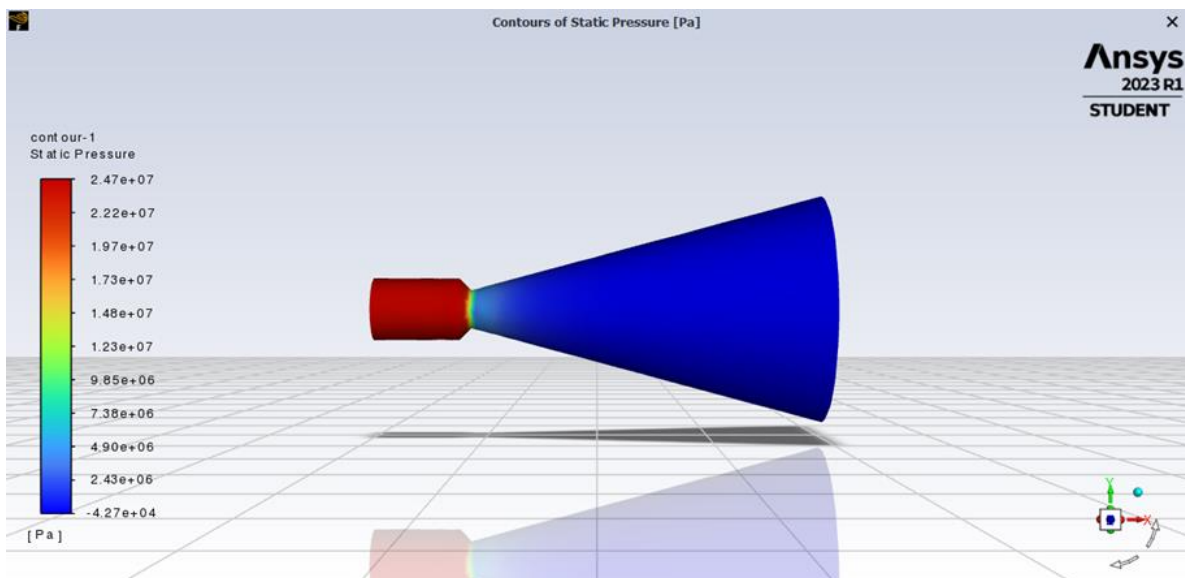
Figure 5.11: Raptor 1 C – D Nozzle Minimum Static Gauge Pressure

- Cone Nozzle:
  - o Minimum static gauge pressure (outlet): -41587.56 Pa
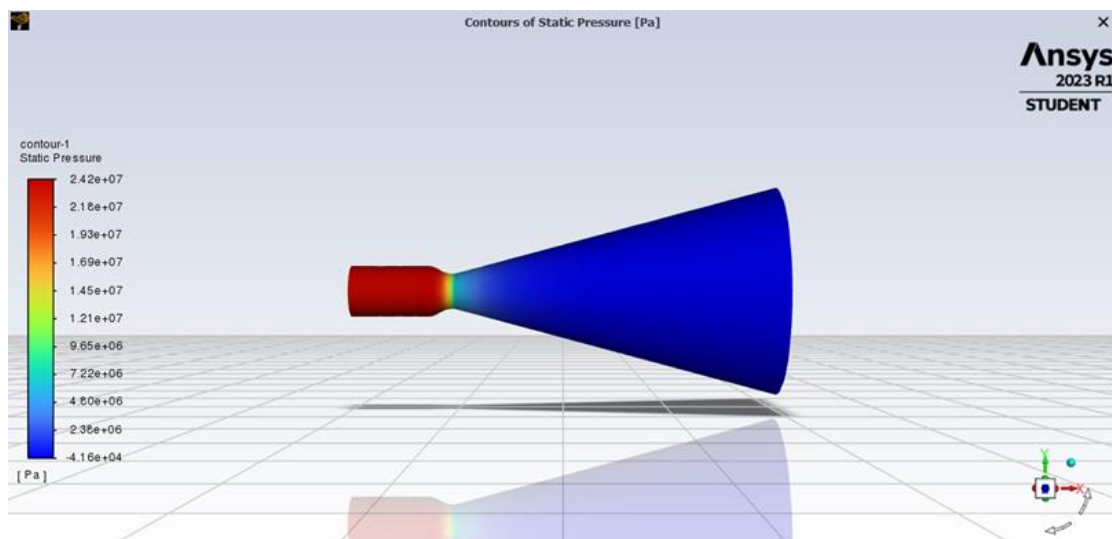
Figure 5.12: Raptor 1 Cone Nozzle Minimum Static Gauge Pressure

- Bell Nozzle:
  o Minimum static gauge pressure (outlet): -58628.36 Pa

Figure 5.13: Raptor 1 Bell Nozzle Minimum Static Gauge Pressure

For this last parameter, the bell nozzle reaches the lowest gauge pressure out of the three engines.

5.3.   Raptor 2

The same process was done again for the Raptor 2 engines, comparing the C-D Nozzle and the Bell Nozzle.

5.3.1. Geometry and Mesh
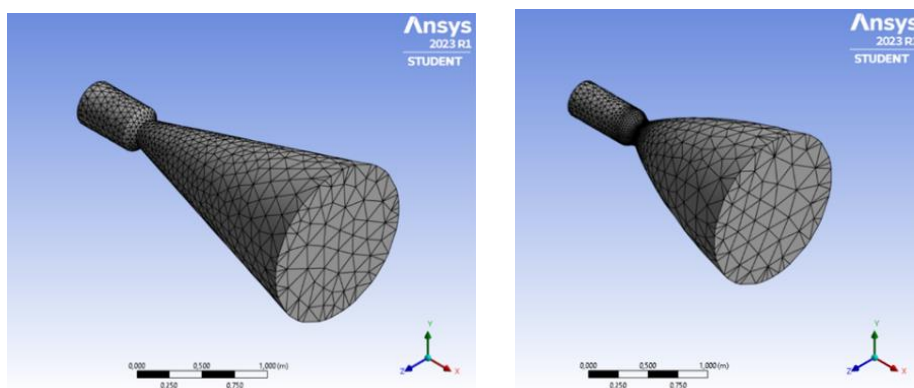
Figure 5.14: Raptor 2 C – D, and Bell Nozzle Geometry

5.3.2. Fluent Settings

The model settings were left the same as the Raptor 1 case study (inviscid flow, energy model turned on), the only changes were the boundary conditions at the inlet and the outlet, as well as the ideal gas properties given by the CEA outputs ($c_p = 2346.7 \frac{J}{kg \cdot K}$, $M_M = 22.080 \frac{g}{mol}$).

5.3.3. Results and Comparison

Once the solution was completed, it was possible to display the contour of some physical quantities of interest, such as velocity magnitude, static temperature and static pressure.

Velocity magnitude and Mach number

In the following contours we can see the progress of the flow velocity for the different engines:

- C-D Nozzle:
    - Maximum velocity magnitude (outlet): 3281.678 m/s
    - Maximum Mach number (outlet): 4.07
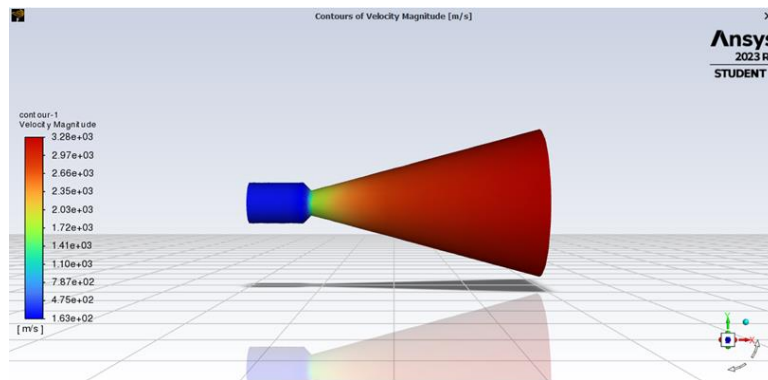
Figure 5.15: Raptor 2 C – D Nozzle Maximum Velocity Magnitude

- Bell Nozzle:
    - Maximum velocity magnitude (outlet): 3342.631 m/s
    - Maximum Mach number (outlet): 4.28
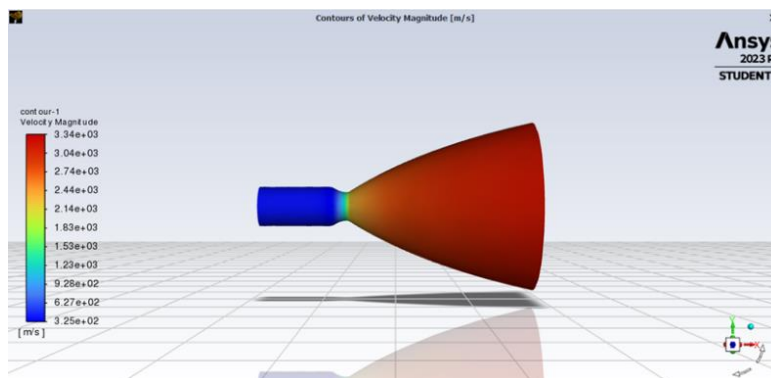
Figure 5.16: Raptor 2 Bell Nozzle Maximum Velocity Magnitude

As we can see, even for the Raptor 2 the bell nozzle is the most efficient engine when it comes to the velocity magnitude at the outlet, improving it from the C-D by +1.86 %.

<u>Static Temperature</u>

Here are the graphics of the progress of static temperature in the two engines along the X axis of the motor.

- C-D Nozzle:
    o Minimum static temperature (outlet): 1447.063 K
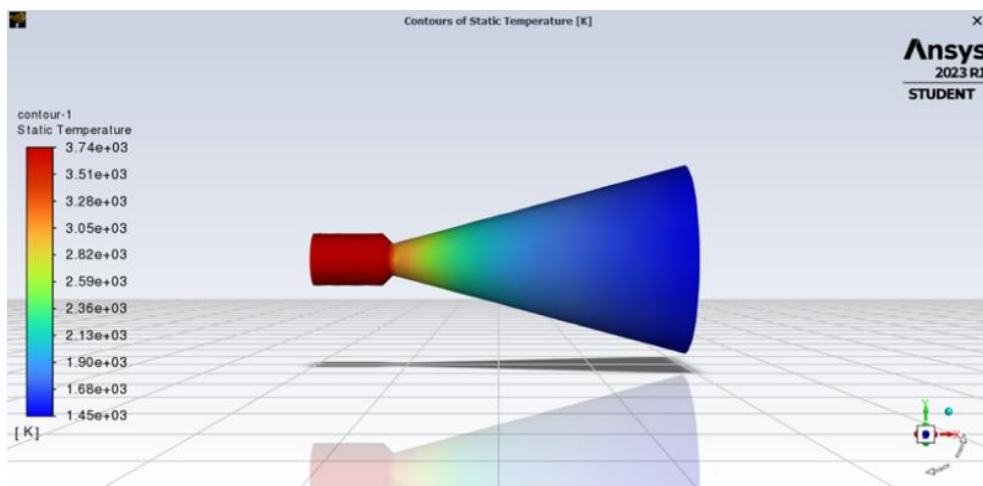
Figure 5.17: Raptor 2 C – D Nozzle Minimum Static Temperature

- Bell Nozzle:
    o Minimum static temperature (outlet): 1361.025 K
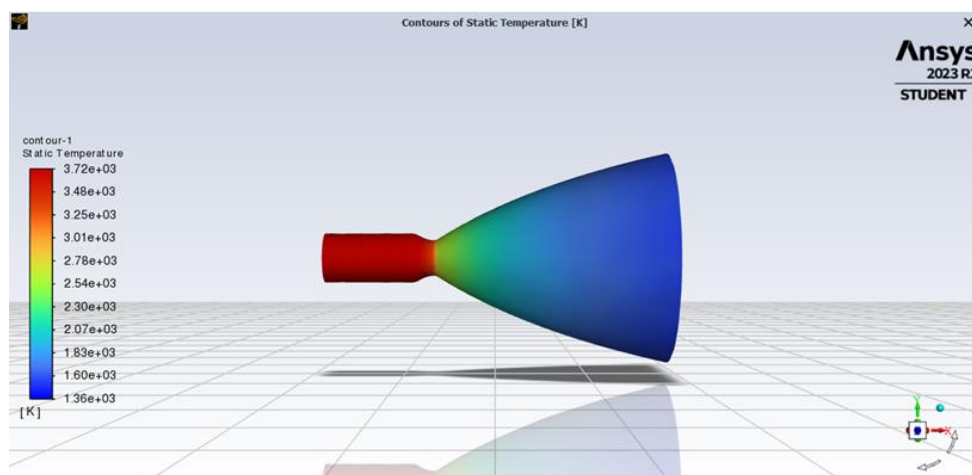
Figure 5.18: Raptor 2 Bell Nozzle Minimum Static Temperature

Even for the Raptor 2, the bell nozzle proves to be the one reaching the overall minimum static temperature of the two engines, lowering it by -5.95 % from the C-D Nozzle case.

<u>Static Pressure</u>

Here are the contours for the progress of static pressure in the two engines.

- C-D Nozzle:
    - o Minimum static gauge pressure (outlet): -28108.6 Pa
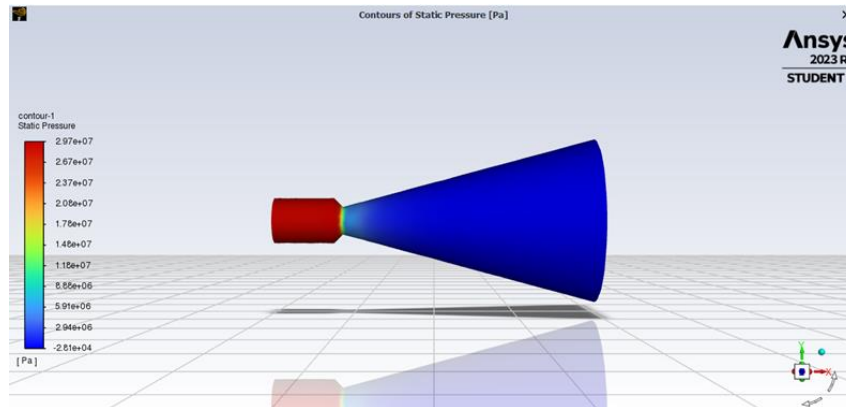
Figure 5.19: Raptor 2 C – D Nozzle Minimum Static Gauge Pressure

- Bell Nozzle:
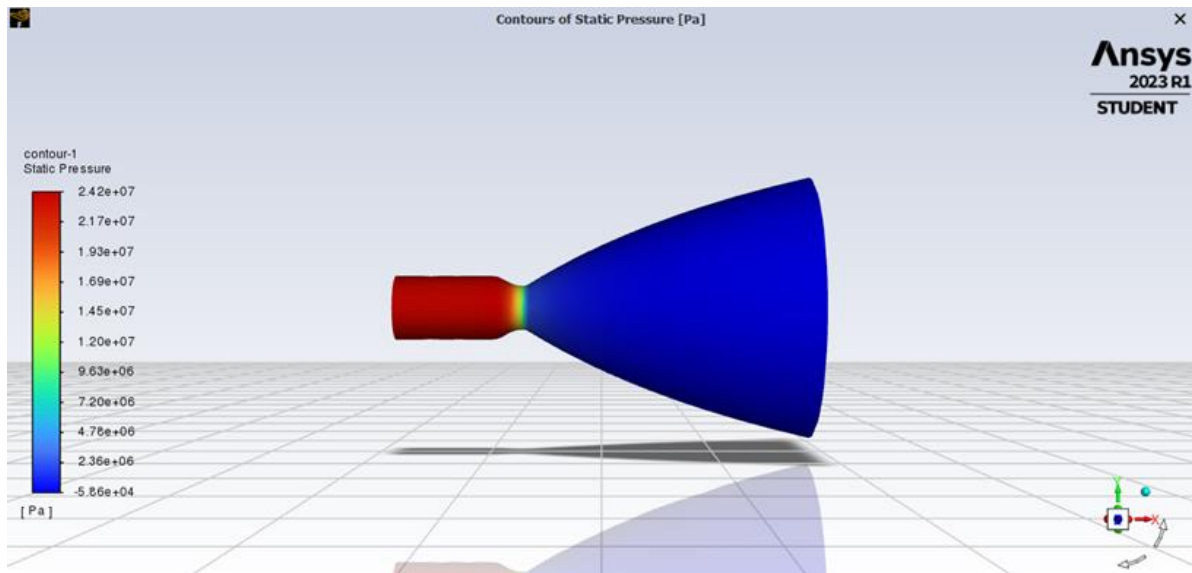   - o Minimum static gauge pressure (outlet): -54421.21 Pa
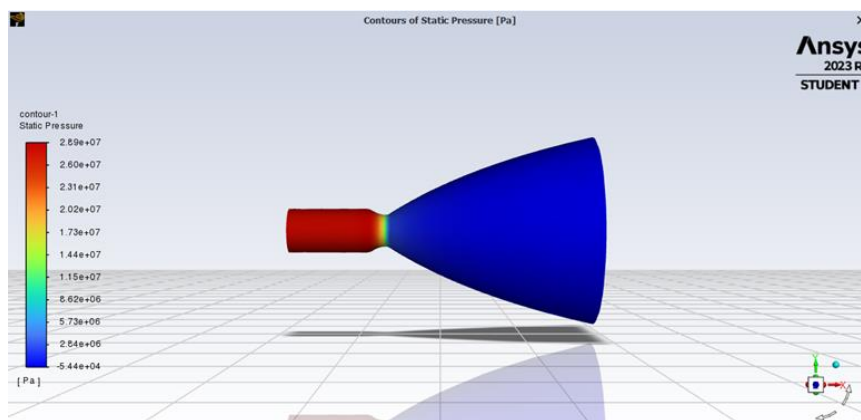
Figure 5.20: Raptor 2 Bell Nozzle Minimum Static Gauge Pressure

At last, also for the static pressure, the bell nozzle proves to be the engine that reaches the lowest value.

5.4.   Comparison between Raptor 1 and 2 bell nozzle engines

In the previous paragraphs, it has been shown that the bell nozzle engines have the best performances regarding the velocity of the flow exiting the nozzle.

In this paragraph, we take a look on how the Raptor 2 has improved performances from its predecessor, the Raptor 1, looking at the two bell designs.
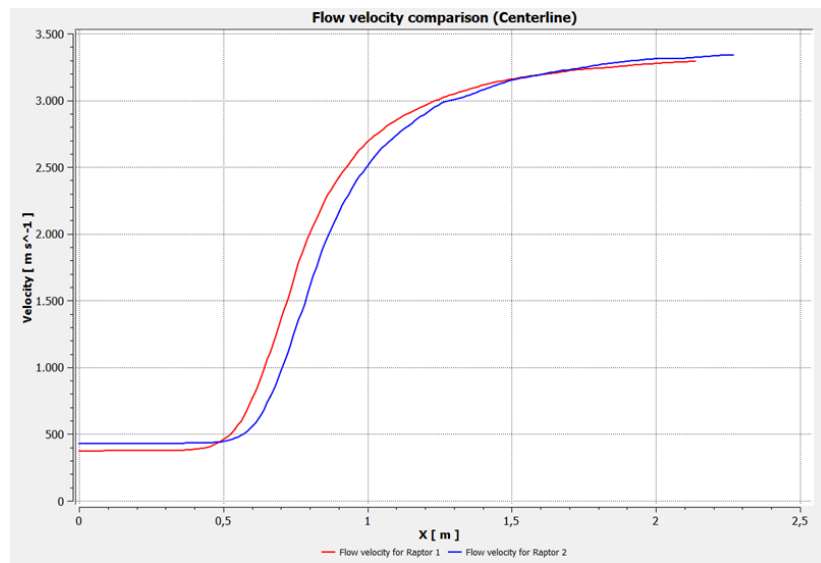
Graph 5.1: Velocity Magnitude
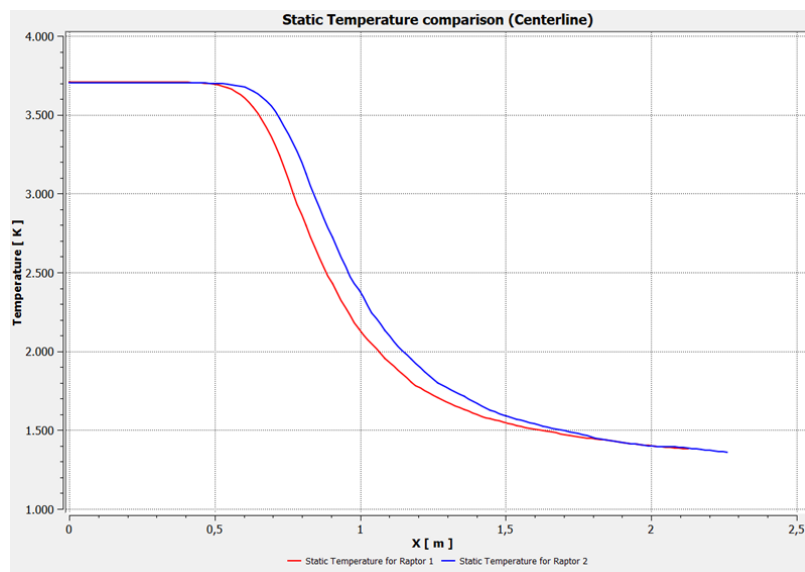
Graph 5.2: Static Temperature

As we can see, the trend for both velocity and temperature along the centreline are similar for the two engines, but the Raptor 2 provides a slightly superior flow speed at the exit section and a slightly smaller static temperature.

In conclusion, we can say that this study showed that the best possible geometry choice for the engine is a bell nozzle, which provides better performances, such as thrust, due to the higher speed of the flow at the exit section.

In addition to that, the analysis also shows how the Raptor 2 increases performances from its predecessor, the Raptor 1, by having a faster flow at the exit which, added to a bigger mass flow rate (from 530.5 to 681.89 kg/s), gives a much bigger thrust to the new version of SpaceX's engine.

6   Cycle Analysis

The Raptor engine utilizes a specific cycle known as the full flow staged combustion. This cycle represents the highest level of technology and complexity, and only three engines have ever demonstrated the full flow staged combustion cycle.

In the 60's, the Soviets developed an engine called the RD-270, which never flew. In the early 2000's, Aerojet and Rocketdyne worked on an integrated powerhead demonstrator, which, again, never made it past the test stand. And the third attempt at developing a full flow staged combustion cycle engine is SpaceX's Raptor engine which was the first to leave the test stand and fly.

In this chapter, we will explore its main components, including tanks, turbopumps, cooling system, and injectors, while describing the functioning of the engine cycle and attempting to size it.

Due to the lack of data, making a comparison between the two versions and updates has been impossible. As a result, all the results in this chapter are based on calculations for the Raptor 2 engine.

6.1.   Engine description

The Raptor engine is a bipropellant engine that utilizes cryogenic liquids. It uses methane as fuel and oxygen as an oxidizer. The Raptor engine follows a staged combustion cycle, a type of combustion cycle where the propellants experience different phases of combustion. Typically, the propellants pass through a small combustion chamber called the pre-burner, where a small portion is partially combusted. The high-energy gas flow then drives a turbine, which serves to power the initial pump that extracts the propellant from the tank. Subsequently, the combusted gas is injected into the main combustion chamber where it undergoes complete reaction with the other liquid component.

In this way, we can achieve higher thrust, but it introduces a lot of engineering challenges, such as managing higher pressure and very hot gases in the plumbing and turbines. For this reason, engineers usually use only one pre-burner and a turbopump system to handle the complexity.

However, SpaceX's Raptor engine takes a different approach. It features a full flow staged combustion cycle, which means that the propellant tanks feed two pre-burners—one running a fuel-rich mixture and the other running an oxygen-rich mixture.

One of the benefits of the full-flow staged combustion cycle is an increased thrust due to the generation of a higher mass flow. Compared to a traditional staged cycle, for the same level of thrust, we can generate more mass, resulting in lower temperatures leading to a longer engine life and higher reliability. As we can see in Figure 6.1 for the same amount of work required, the FFSC(Full-Flow Staged Combustion Cycle) has more mass flow and a minor deltaT which means that the turbines

can run cooler and at lower pressures because the ratio of fuel and oxidizer needed to spin the turbopumps is much lower.

We can compare this closed cycle with the oxidizer rich and the fuel rich closed cycles, helped by the sequent image:

Figure 6.1: Comparison of cycles in terms of temperature

With a full flow cycle all the fuel and all the oxidizer go through the preburners. As much propellant as necessary can be burned to power the turbopumps, but the ratios will be incredibly fuel rich and oxygen rich, such that the temperatures at the turbines will be much lower and this is translated in longer lifespans for the turbopump assembly. Another consequence is that more combustion happens in the combustion chamber and less in the preburner, so more gas-gas combustion and more efficiency.

Now let's take a closer look at how the cycle works, thanks to an unofficial schematic found on dedicated discussion forums (see Figure 6.2).
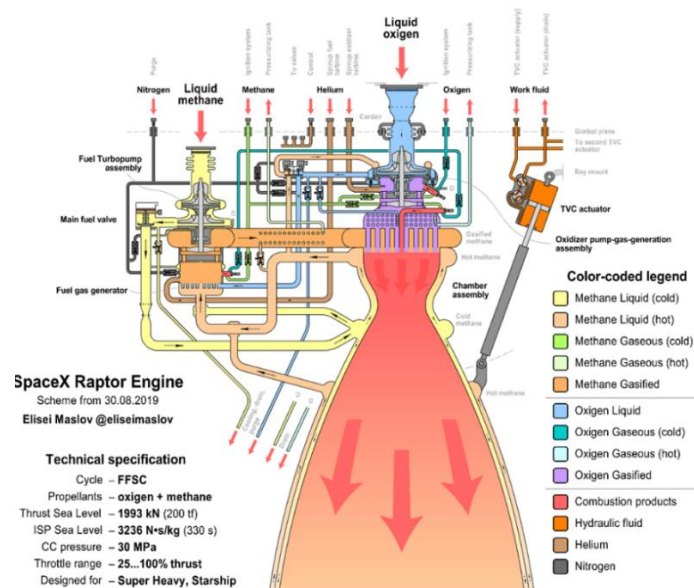

Figure 6.2: Complex Raptor 2 schematic

Let's follow the path of the two liquids, starting with methane.

Liquefied methane starts from its own tank and is pumped into the nozzle cooling system by a two-stage pump. In the preburner, the still-liquid but warmer methane reacts with a small amount of liquid oxygen (typical OF about 0.20-0.30) to create a hot gaseous mixture (about 900 K) called fuel-rich. To promote combustion, the two liquids are injected into the preburner through injectors, which atomize the fuel. The high-pressure gas powers a turbine and the methane pump system. Next, the fuel-rich gas reaches the main combustion chamber, where it is injected through swirl injectors (see paragraph 6.6).

Similarly, let's examine the path of oxygen. It is also pumped by a single-stage pump directly into the preburner, where it is atomized with injectors. Here, it reacts with high OF ratios (about 40-55) to create a gaseous mixture called ox-rich. The gas drives a turbine and is finally injected into the combustion chamber through injectors.

As shown in the diagram, we also have other working gases like nitrogen and helium. Both are inert gases, meaning they react minimally with other substances. These gases are used during the engine startup phase. The high-pressure storage in the tanks, when released through servo valves, sets the turbines in motion, which then activate the pumps. Additionally, they are often used during purging and chill down phases, where the system is cleared of residues (like air or remnants of previous combustion) and conditioned to handle cryogenic temperature.

6.2.   Sizing of the cycle

In this section we will attempt a preliminary sizing of the steady-state system of the Raptor 2. These calculations required extensive research and time due to the scarcity of data and the complexity of the cycle. In particular, it was difficult to grasp the details and fit them into a more complex framework. However, with the appropriate assumptions, we obtained meaningful and consistent results. SpaceX itself has been developing the raptor engine since 2009 with an entire dedicated department. In an interview, Elon Musk explained that they have tested and melted over 50 engines. Therefore, we are aware that our preliminary and simplified sizing will never match the actual values. However, we hope the results to be a good approximation of the real values.

6.2.1. Model and Assumption

First up, let's simplify the system by reducing its complexity and then introducing initial assumptions.

We have decided to use the Figure 6.2 as a reference, but we omitted the nitrogen and helium system used for cooldown and engine start-up. Additionally, we omitted various control valves, pressure valves, and sensor systems. Furthermore, we did not consider the tank pressurization system. In fact, it seems that some of the liquids undergo a phase change through heat exchangers placed after the two preburners and return to the tank, pressurizing it.
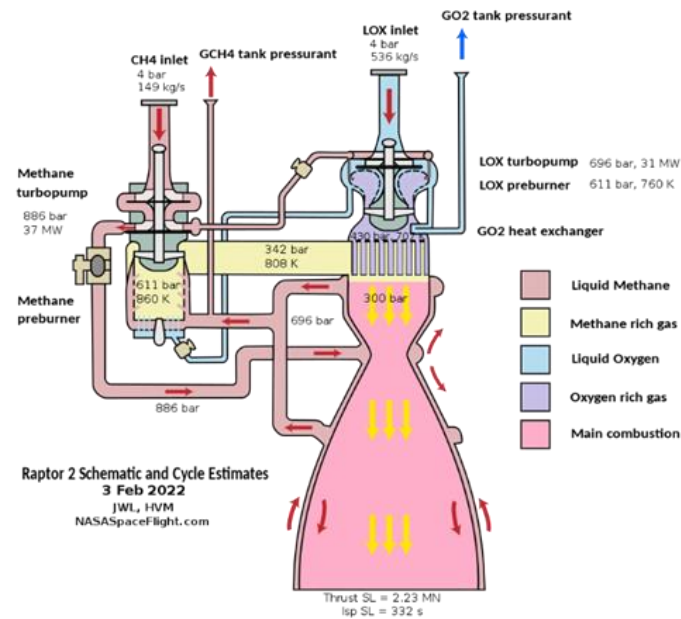
Figure 6.3: Simple Raptor 2 schematic

After these simplifications, we arrived at a considerably less complex system, resembling the one illustrated in Figure 6.3, which we found useful for verifying our calculations.
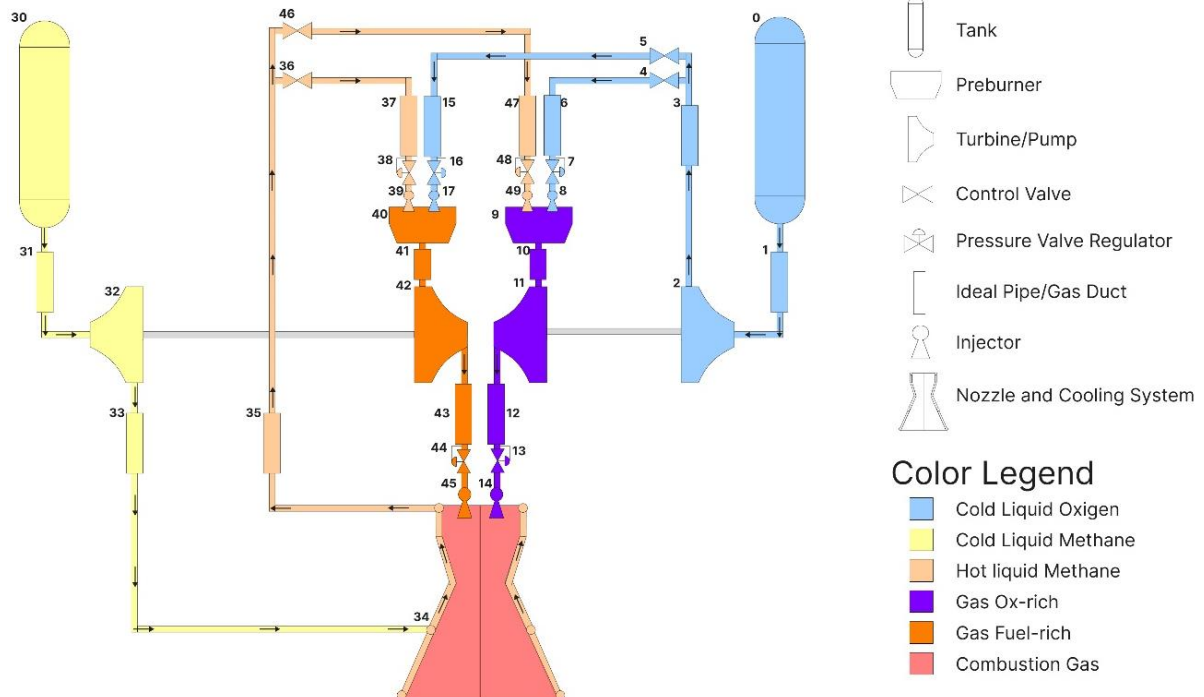

Figure 6.4: Adopted Raptor 2 schematic

Figure 6.4 shows all the components of our simplified version of the cycle.

Let's switch to the initial assumptions on cryogenic liquids, gas and combustion.

The rocket employs liquid methane and liquid oxygen as propellants. We utilized data provided by NIST (National Institute of Standards and Technology) to model their thermodynamic properties. The *"refprom.m"* function in MATLAB has been employed to extrapolate the thermodynamic properties of these pure substances.

The combustion process in the two preburners is calculated using *"CEA.m"*, a MATLAB function based on the CEA (Chemical Equilibrium with Applications) code discussed previously.

The main limitation of the preburner is related to temperature. If the temperature exceeds a certain threshold, the rich gases can cause the two turbines to melt, resulting in engine failure. To mitigate this issue, unconventional oxidizer/fuel ratios are typically employed to achieve non-stoichiometric combustion and promote gas mixing, thereby reducing the temperature. The design of the injector and the preburner combustion chamber is extensively studied to effectively manage the temperature.

Initially, in our model, we utilized the enthalpy-pressure problem from the CEA library. However, we observed that it produced excessively high temperatures when compared to standard parameters with reasonable oxidizer/fuel ratios (about 50:1). Typically, the preburner temperature ranges from 650-850 K for oxidizer-rich configurations and 800-1100 K for fuel-rich configurations, but we obtained above 1300 K for ox-rich and 1500K for fuel-rich. Consequently, we transitioned to the temperature-pressure problem, where we explicitly set the exit temperature of the rich gases. By using the *"CEA.m"* function, we calculated the results of the combustion process and observed a partial reaction of the majority of the gas.

We are aware of the limitations of the chosen model. However, when we used the "tp" (temperature-pressure) approach, we obtained plausible and meaningful results.

Furthermore, at the end of the cycle, we ran the CEA code again, setting the "rocket" problem type and providing the calculated rich gases as inputs. This allowed us to verify the accuracy of our model using data provided by SpaceX.

Finally, we modelled the rich gases (fuel rich and ox rich) as ideal gases, since they follow the general gas equation $p = \rho RT$ and have constant pressure (cp), specific heat at constant volume (cv), and the ratio of specific heats (gamma) are constant.

6.2.2. Initial conditions

One challenging task was to select the appropriate mathematical model for each component and determine their initial and parameter data accurately.

For the modelling part, we followed a procedure from a research paper published by the German Aerospace Centre (DLL). As for the parameters and initial values, we relied on a guide found on a technical blog dedicated to the RPA software, which was also used in the previous chapter.

The first element we encountered in the cycle are tanks for which we could not find any specific information. Since we know that deep cryogenic liquids are used in these tanks, we chose a temperature of 63K for oxygen and 97K for methane and a pressure of 4 bar. At this point, we considered the pipes and the gas duct as ideal, disregarding any pressure losses and friction caused by fluid-wall interactions. Next, there is the turbopump system, consisting of three main elements: the pump, the shaft, and the turbine. The pump and turbine utilize a polytropic transformation, expressed by the following formulas:

$$PUMP: h_2 = h_1 + \frac{h_2' - h_1}{\eta_s} \quad TURBINE: h_2 = h_1 + \eta_s(h_2' - h_1)$$

Where h_1 e h_2 are the real enthalpy, h_2' is the ideal enthalpy after transformation and η_s is the isentropic efficiency. Thinking that the turbine works with an ideal gas as the working fluid, we can use $h = c_p T$ and see:

$$T_2 = T_1 + \eta_s(T_2' - T_1)$$

The component model of the shaft currently calculates and establishes the power balance of the turbopump in the cycle analysis. Additional efficiencies beyond those of the turbine and pump are considered to account for gear losses, leakage, and other factors:

$$P_{pump} = \{\dot{m}|\Delta h|\}_{\{pump\}} = \eta_{mecc}\{\dot{m}|\Delta h|\}_{turb}$$

The efficiencies of the turbopump system vary significantly depending on the system characteristics and the working fluid. We selected typical values based on the information presented in the blog (see table).

The cooling system was modelled as a simple heat exchanger with a significant imposed pressure drop, although it will receive further dedicated analysis. An empirical formula, $\Delta p = 0.35 p_c$, provides an estimate of the pressure loss.

For the valves and injectors, we used typical values. Specifically, we examined in depth the injectors in a separate section, where we estimated the required pressure losses for their operation ($\Delta p = 46$ bar). For simplicity, we assumed that the injectors in the main combustion chamber and those in the two preburners are identical.

To summarize, we have compiled all the chosen and utilized values into a table.

Table 6.1: Starting data for cycle analysis

Object	Data		
Tank Ox	$T_{tankO} = 63$ K	$P_{tankO} = 4$ bar	
Tank CH4	$T_{tankF} = 97$ k	$P_{tankF} = 4$ bar	
Turbopump Ox	$\eta_{turbine} = 0.72$	$\eta_{pump} = 0.75$	$\eta_{mecc} = 0.98$

Turbopump CH4	$\eta_{turbine}$ = 0.65	η_{pump} = 0.7	η_{mecc} = 0.98
Preburner Ox	T = 750 K	Δp = 0.95	O/F = 50
Preburner CH4	T = 950 K	Δp = 0.95	O/F = 0.22
Cooling System	Δp = 105 bar		
Injector	Δp = 46 bar		
Valve	Δp = 15 bar		
Main Chamber	$\dot{m}_p$ = 681.89 kg/s	P_c = 300 bar	O/F = 3.4

6.2.3. Calculations and results

The algorithm searches for the required pumping pressures to ensure the maximum thrust operation of the cycle. The code utilizes two loops cycle to find the output pressures in the main chamber at 300 bar with an accuracy of 1 bar (0.33% error). The first loop assumes a pumping pressure for the Ox branch and, through a series of sequential steps, determines the LOX conditions at the inlet of the preburners (in Figure 6.4: ox_main branches 0-8 and ox_supply branches 5, 15, 16, 17). Then, the second loop begins, calculating the entire CH4 branch (from number 30 to 49) starting from a p_ch4_guess and iterating until convergence (p_rox_46 = 300 bar). At this point, the first loop concludes by calculating the remaining part of the Ox system (from 8-14) until achieving p_rch4 = 300 bar.

Let's examine the results obtained with p_ox_guess = 640 bar and p_ch4_guess = 750 bar, with an incremental increase of p_guess + 3 bar between iterations.
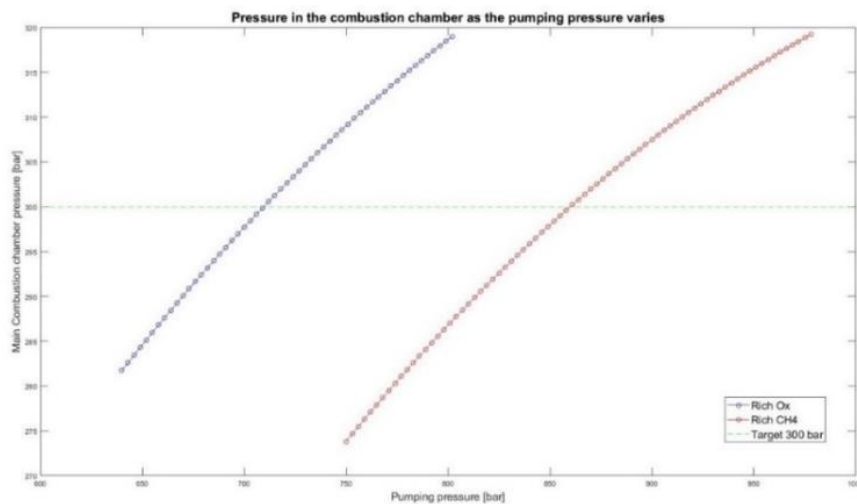
Graph 6.1: Pressure in the combustion chamber

In the Graph 6.1: Pressure in the combustion chamber we plotted the pressure in the combustion chamber as the pumping pressure varies. The cycle converges with $pumping\_ox = 704\ bar$ and $pumping\_ch4 = 837\ bar$. Analyzing the graph we discovered a nonlinear trend that demonstrates a difficulty to achieve higher pressure in the main chamber that improves the efficiency of the rocket.
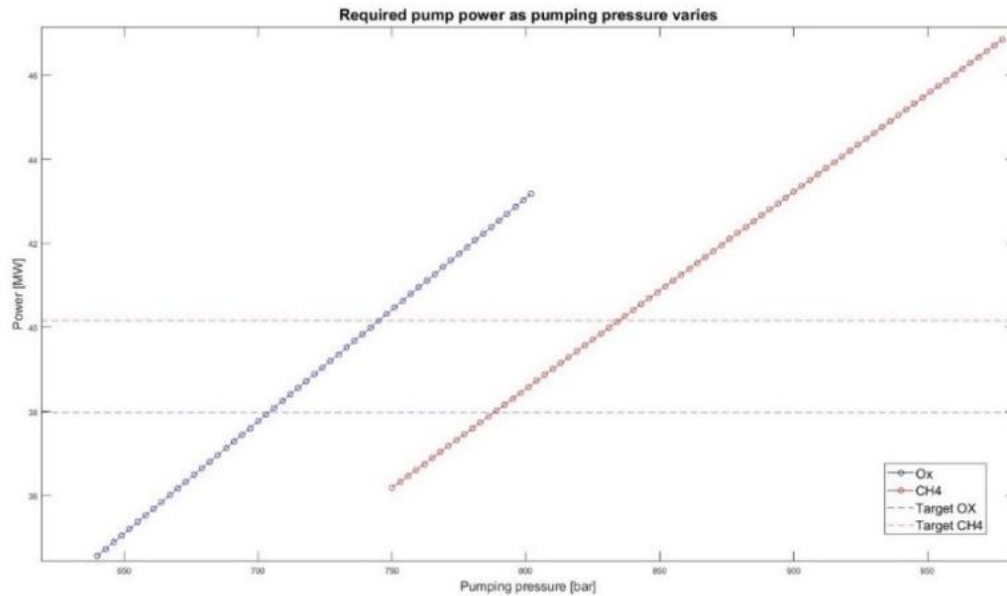
Graph 6.2: Required pump power

In the Graph 6.2: Required pump power we plotted the required pump power as the pumping pressure varies. The cycle converges with $pumping\_power\_ox = 37.97\ MW$ and $pumping\_power\_ch4 = 40.16\ MW$. The amount of power required is very high and increases with the rising pressures at play. We will delve deeper into the turbopump system in a dedicated paragraph.

The next image is dedicated to the result of the calculation of the code. The schematic resumes the most important parameter of each component.

Figure 6.5: Calculation of Raptor 2

Calculation of Raptor 2

0. Tank LOX:
p = 4 bar
T = 63 K
m = 526.91 kg/s

1. Ideal Pipe
p = 4 bar
T = 63 K
m = 526.91 kg/s

2. Pump:
dp = +700 bar
W = 37.97 MW
eta = 0.75

3. Ideal Pipe
p = 704 bar
T = 80.85 K
m = 526.91 kg/s

5. Control Valve:
dp = -15 bar
m_supply = 31.91 kg/s

4. Control Valve:
dp = -15 bar
m_main = 494.99 kg/s

6. Ideal Pipe:
p = 689 bar
m = 494.99 kg/s

8. Injector:
dp = -46 bar
T = 80.21 K
m = 494.99 kg/s

9. Preburner OX-rich:
p = 643 bar
T = 770 K
O/F = 50
dp = 0.95%

11. Turbine:
dp = -265.63 bar
eta = 0.72

12. Gas Duct:
p = 345.21 bar
T = 698.89 K
m = 504.89 kg/s

14. Injector:
dp = -46 bar

Main Chamber:
p = 300 bar
T = 3630 K
c* = 1823.28 m/s
m = 681.89 kg/s
Is = 334 s

15. Ideal Pipe:
p = 689 bar
m= 31.91 kg/s

47. Ideal Pipe:
p = 717 bar
m = 9.90 kg/s

10. Gas Duct:
p = 610.85 bar
m= 504.89 kg/s

41. Gas Duct:
p = 637.45 bar
m= 176.99 kg/s

36. Ideal Pipe:
p = 717 bar
m = 145.07 kg/s

38. Injector:
dp = -46 bar
T = 283.81 K
m = 145.07 kg/s

40. Preburner F-rich:
p = 671 bar
T = 950 K
O/F = 0.22
dp = 0.95%

42. Turbine:
dp = -291.89 bar
eta = 0.65

43. Gas Duct:
p = 345.55 bar
T = 905.60 K
m = 176.99 kg/s

45. Injector:
dp = -46 bar

34. Cooling Jacket:
dT = + 153 K
dp = -105 bar

m_ox.main = 495 kg/s
m_ox.supply = 32 kg/s
m_ch4.supply = 9.90 kg/s
m_ch4.main = 145 kg/s

46. Control Valve:
dp = -15 bar
m_supply = 9.90 kg/s

36. Control Valve:
dp = -15 bar
m_main = 145.07 kg/s

32. Pump:
dp = +833 bar
W = 40.16 MW
eta = 0.70

35. Ideal Pipe
p = 732 bar
T = 288 K
m = 154.97 kg/s

33. Ideal Pipe:
p = 837 bar
T = 135.26 K
m = 154.97 kg/s

30. Tank LCH4:
p = 4 bar
T = 97 K
m = 154.97 kg/s

31. Ideal Pipe
p = 4 bar
T = 97 K
m = 154.97 kg/s

Finally, here are the results obtained from the combustion of the two gas-rich fuels. The combustion takes place at the designed pressure of 300 bar. The NASA function solve the "rocket" problem by using an input expansion ratio of 34.34 for Ae/At, along with gas mixtures calculated by the CEA for the preburners reaction. Now, let us examine the combination of the two gas-rich blends.

Table 6.2: Fuel rich gas mixture (RCH4)

Element	Mass Fraction
CO	70,24%
CO2	0,54%
C2H6	3,05%
C3H8	0,13%
H2O	0,97%
C(gr)	17,47%
CH4	7,61%

Table 6.3: Oxidizer rich gas mixture (ROX)

Element	Mass Fraction
CO2	5,38%
H2O	4,40%
O2	90,22%

The O/F ratio in the main combustion chamber is 2.85 ($\frac{m_{rox}}{m_{rch4}}$), but if we consider only the masses of O2 and CH4 that make up the two mixtures, the O/F ratio increases to approximately 3.6. Now let us look at the properties of the combusted gases calculated by CEA. Specifically, we will examine the data calculated at the end of combustion (Comb End), at the throat and at the exit.

Table 6.4: Combustion gas parameters

Symbol	Comb End	Throat	Exit
P (bar)	300	171.72	0.76
T (K)	3630.60	3393.23	1430.43
Density (kg/m^3)	22.0158	13.597	0.1462
Gamma (cp/cv):	1.1566	1.1595	1.2157
Sound Velocity (m/s):	1255.4	1210.1	796.9
Mach Number	0	1	4.112

In the table below, we present a straightforward comparison between the main parameters of Raptor 1 and Raptor 2, calculated using the CEA. For Raptor 1, we used the same code as before, keeping identical efficiency parameters, and disregarding any potential improvements between the two versions. The only values that have been altered in the Raptor 1 code are the overall mixture ratio of

OF = 3.6, the mass flow rate of propellant gases of m = 530.1 kg/s, the combustion chamber pressure of 250 bar, and the Ae/At ratio of 35.

	Raptor 1		Raptor 2	
	Throat	**Exit**	**Throat**	**Exit**
Ae/At:	1	35	1	34.34
C* (m/s):	1823.38	1823.38	1823.28	1823.28
C_f **(ideal)**	0.66072	1.8085	0.66368	1.79718
C_f **(vac)**	1.23494	1.89833	1.23608	1.88462
I_{sp} **(vac) (s)**	229.61	352.96	229.81	350.39
I_{sp} **(s)**	122.85	336.25	123.39	334.13
T (tons)		178.25		227.84

SpaceX doesn't provide exact data, but in the image {ref}, some parameters are provided from sources closely associated with SpaceX. Our values have comparable figures to those shown in the image, with an error of approximately 2-3%, likely due to dissipative effects or due to model error.
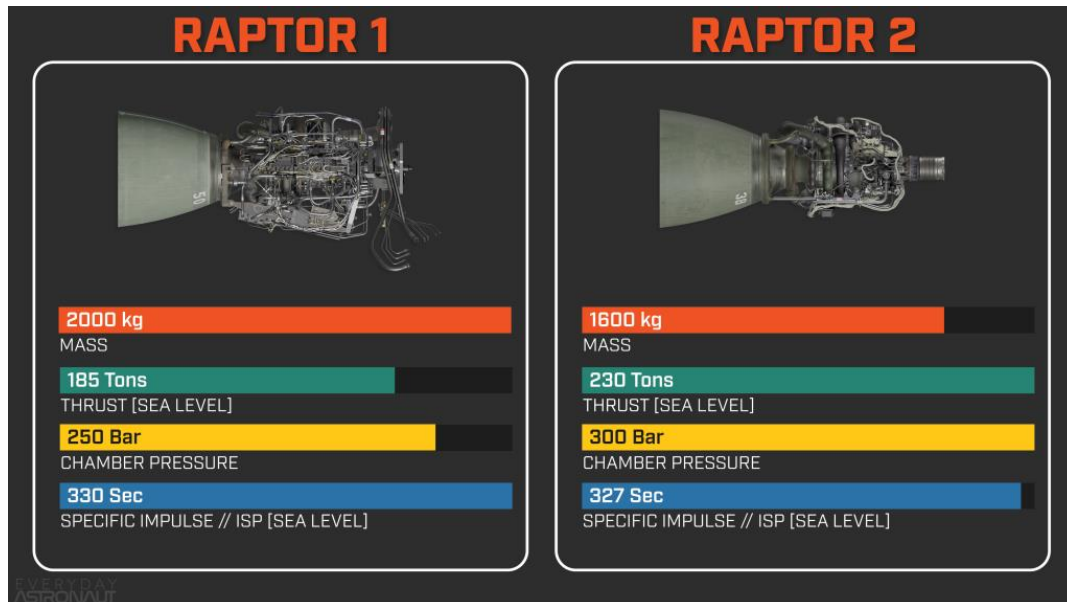

Figure 6.6: Main propulsion parameters of Raptor engine

As we can see, Raptor 2 produces approximately 25% more thrust compared to the previous version, though it comes with a reduction in specific impulse.

6.3. Tank

The liquid oxygen (LOX) and liquid methane (LCH4) are stored into two different tanks. These tanks are thermally isolated and pressurized. The properties of the LOX are:

$$T_{tankOX} = 63\ K \quad P_{tankOX} = 4\ bar \quad \rho_{LOX} = 1269.18 \frac{kg}{m^3}$$

Instead, the properties of the fuel are:

$$T_{tankF} = 97\ K \quad P_{tankF} = 4\ bar \quad \rho_{LCH4} = 443.27 \frac{kg}{m^3}$$

The dimensioning of the fuel and oxidizer tanks must be done by considering a safety margin due to a reasonable deviance of the fuel consumption for the expected mission and due to a normal leftover in the system pipes and tanks. For these reasons a safety factor has to be used: $K_s = 1.05$. Using the LCH4 feed, the LOX feed and the burning time (supposed 300 s) it can be calculated the mass of fuel and oxidizer:

$$M_{LCH4} = \dot{m}_f \cdot t_b \cdot K_s = 4.8817 \cdot 10^4\ kg$$

$$M_{LOX} = \dot{m}_o \cdot t_b \cdot K_s = 1.6598 \cdot 10^5\ kg$$

Dividing these for each density it can be obtained:

$$V_{LCH4} = \frac{M_{LCH4}}{\rho_{LCH4}} = 110.1295\ m^3$$

$$V_{LOX} = \frac{M_{LOX}}{\rho_{LOX}} = 130.7760\ m^3$$

The pressurization is supposed to be given by helium. The helium's properties are:

$$\gamma_{He} = 1.66 \quad R_{He} = 2078.6 \frac{J}{kg \cdot K} \quad T_{He_i} = 290\ K$$

From these results other propulsive parameters can be obtained:

$$I_v = \rho_{AV} \cdot I_{sp} = 2.9156 \cdot 10^5 \frac{kg}{m^3} \cdot s$$

$$I_{tot} = I_{sp} \cdot (M_{LCH4} + M_{LOX}) \cdot g_0 = 6.8904 \cdot 10^8\ N \cdot s$$

It is supposed that a single tank is used for the pressurization of the oxidizer and another single tank for the pressurization of the fuel, because the oxidizer and the fuel are at two different temperatures. This could increase the weight, because different tanks are used for the same thing, on the other hand, it could reduce the length of the tubes, positioning every tank near the one that it pressurized.

The procedure for the sizing of the helium tanks is the same for each of the two tanks. The starting pressure for the helium is calculated with this equation:

$$P_{He_i} = P_{tank} \cdot \left(\frac{T_{He_i}}{T_{tank}}\right)^{\frac{\gamma_{He}}{\gamma_{He}-1}}$$

Then, an iterative method is applied to calculate the mass and the volume required by the helium. This method calculates the mass and the volume at every iteration. The starting volume for the helium at the beginning of the method is supposed to be 0. The equations used are:

$$M_{He}(i) = \frac{P_{tank}}{T_{tank} \cdot R_{He}} \cdot \left(V + V_{He}(i-1)\right) \quad V_{He}(i) = \frac{M_{He}(i)}{\rho_{He}} = \frac{M_{He}(i)}{P_{He_i}} \cdot T_{He_i} \cdot R_{He}$$

The method stops when the toleration reaches the limit required:

$$toll = \frac{M_{He}(i) - M_{He}(i-1)}{M_{He}(i)} < 1 \cdot 10^{-5}$$

It is illustrated on the MatLab file *"RaptorTank.m"*. The results obtained are:

$$M_{He_O} = 320.4059 \; kg \qquad V_{He_O} = 30.7282 \; m^3$$

$$M_{He_F} = 373.3342 \; kg \qquad V_{He_F} = 12.0925 \; m^3$$

6.4. Turbopumps system

In this paragraph, we will examine the turbopump system using the assistance of an unofficial model (Figure 6.8 e **Error! Reference source not found.**). We will explore some important aspects of this vital system and the challenges involved in the project.

A turbopump is a precise and high-speed rotating device typically comprised of a gas turbine that drives one or two centrifugal pumps. Its purpose is to extract propellants from the vehicle's tanks, increase their pressure, and deliver them into the appropriate piping systems. SpaceX has developed two separate turbopump systems:
- Oxidizer turbopump
- Fuel turbopump

6.4.1. Pump

The propellant enters the pump through an inducer, which is a specialized spiral flow impeller. The inducer slightly elevates the propellant's pressure, around 5 to 10% of the total pressure increase. This slight pressure boost ensures that cavitation is avoided when the flow enters the main pump impeller. Then, the fluid enters the axial-flow pump, where alternating rotating and static blades progressively raise its pressure. Most of the kinetic energy given to the flow by the pump impeller is converted into hydrostatic pressure in the diffusers.

The fluid enters the impeller, which is essentially a wheel with spiral curved vanes rotating within a casing. The fluid gets accelerated within the impeller channels and leaves its outer edge with a higher velocity. It then enters the collector and subsequently enters the diffuser, where it converts from kinetic energy (velocity) to potential energy (pressure).

Typically, LOX (liquid oxygen) pumps have single-stage impellers, while fuel pumps have multistage impellers with two or three impellers arranged in series.

It is possible to predict the pump's performance at different speeds if its performance is known at any given speed. Now some important variables can be introduced:

- N is the rotation of the shaft in [rad/s] or [rpm]
- Q is the flow rate in [m^3/s]
- H is the pump head in [m]. It is the maximum height that the pump can achieve pumping against gravity. (If Δp is the discharge pressure, then using the Stevino's law $H = \frac{\Delta p}{\rho g}$)

N, Q, and H are related to each other through proportional relationships. This relationship allows us to derive a dimensionless parameter called the specific speed N_s, which is very useful for choosing the best geometry and comparing different pumps.

$$N_s = N \frac{\sqrt{Q_e}}{(g_0 \Delta H_e)^{3/4}}$$

The calculation of N_s requires studying and utilizing the condition of maximum efficiency (denoted by the subscript "e"). For each range of specific speed, only certain shapes and impeller geometries proved most efficient, as shown in Figure 6.7.
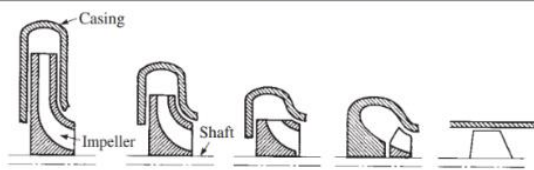

	Impeller type				
	Radial	Francis	Mixed Flow	Near Axial	Axial
Basic shape (half section)					
Specific speed N_s					
U.S. nomenclature	500–1000	1000–2000	2000–3000	3000–6000	Above 8000
SI consistent units	0.2–0.3	0.4	0.6–0.8	1.0–2.0	Above 2.5
Efficiency %	50–80	60–90	70–92	76–88	75–82

Figure 6.7: Pump Type Samples, Range of N_s, Efficiency

The impeller tip speed in centrifugal pumps is limited by design and material strength considerations and ranges between 200 to 450 m/sec. This maximum impeller tip speed determines the maximum head that can be obtained from a single stage. The impeller vane tip speed u_{tp} is the product of the shaft speed, expressed in radians per second, and the impeller radius and is related to the pump head ΔH by

$$u_{tp} = k \sqrt{2g_0 \Delta H}$$

Where k is a velocity correction factor (0.9-1.1).

The mass flow rate $\dot{m}$ is used to define the impeller inlet and outlet area using the equation of continuity $\dot{m} = A_1 v_1 \rho_1 = A_2 v_2 \rho_2$. Typical values of inlet velocity are between 2 and 6 m/s, instead for outlet velocity are from 3 to 15 m/s.

Pump performance is limited by cavitation, a phenomenon that occurs when the static pressure of a fluid at any point in a pipe becomes less than the fluid's local vapor pressure. These bubbles collapse when they reach regions of higher pressure, that is, when the static pressure in the fluid is above the vapor pressure.

Bubbles that travel along the pump impeller surface from the low-pressure region (at the leading edge of the vane where they are formed) downstream to the higher-pressure region collapse. These sudden collapses create local high-pressure pulses that may cause excessive stresses and erosion at the impeller surface.

The required suction head H_R is the limit value of the head at the pump inlet (above the local vapor pressure); below this value cavitation in the impeller may occur.

Usually, $H_R = 80\% H_A$, where H_A is often abbreviated as NPSH (Net Positive Suction Head) and is the maximum head available for suppressing cavitation at the inlet to the pumps:

$$NPSH = H_{tank} + H_{elevation} - H_{friction} - H_{vapor}$$

The required suction head above vapor pressure can be determined from the suction-specific speed S and the volume flow rate Q_e at maximum efficiency:

$$S = 21.2N \frac{\sqrt{Q_e}}{NPSH^{0.75}}$$

The suction-specific speed S depends on the design quality and the specific speed N_s. When using ft-lbf units, the suction-specific speed S ranges from 5000 to 60000. Pumps with poor suction characteristics have values closer to 5000. Inducers are now designed to run steadily with abundant vapor bubbles near the leading edge of their vanes, but these bubbles collapse at the trailing end of the vane. Inducers can now operate at S-values above 80000. Considering that the Raptor engine is reusable, we choose an S-value of around 18000.

6.4.2. Preliminary analysis of ox pump

The porpoise of this section is to determine shaft speed and overall impeller dimensions for the oxygen pump using the data calculate in this chapter without considering the inducer.

The initial data are the pressure of the tank $p_{tank} = 4\ bar$, discharge pressure of the pump $p_{pump} = 704\ bar$ and the mass flow $\dot{m} = 527 \frac{kg}{s}$ $(Q = 0.42 \frac{m^3}{s})$.

Using the "refpropm.m" function of NIST we can find the vapor pressure $p_{vapor} = 1499.28\ Pa$ and the density $\rho = 1269.18\ kg/m^3$ at the inlet.

Now we can calculate the various head like $H = \frac{\Delta p_x}{\rho g_0}$ with $g_0 = 9.81\ m/s\text{^}2$.

$$H_{pump} = \frac{p_{pump}}{\rho g_0} = 5622.18\ m \quad H_{tank} = \frac{p_{tank}}{\rho g_0} = 32.13\ m \quad H_{vapor} = \frac{p_{vapor}}{\rho g_0} = 0.12\ m$$

Considering that the tank is 20 m above the engine, we can determinate the NPSH without the head lost for friction

$$NPSH = H_{tank} + H_{elevation} - H_{vapor} = 52.01\ m$$

The required suction head will be taken as 80% of the available suction head in order to provide a margin of safety for cavitation $H_r = 0.80\% NPSH = 41.61\ m$. Assuming a suction specific speed of 18000, we can find the shaft speed:

$$N = S \frac{H_r^{0.75}}{21.2\sqrt{Q}} = 8850.61\ rpm$$

(N.B: for this relation it is necessary to convert from SI system to U.S due to the choice of S).

Now we can calculate the specific speed, using the $\Delta H = H_{pump} - H_{tank} - H_{elevation} = 5570.06\ m$

$$N_s = N\ \frac{\sqrt{Q_e}}{(g_0 \Delta H_e)^{3/4}} = 0.93$$

According to Figure 6.7, the impeller shape for this value of N_s will be the Near Axial.

Assuming the pump efficiency is $\eta = 75\%$, we find that $D_2 = \frac{2u_{tp}}{N\eta} = 0.86\ m$ with the tip speed:

$$u_{tp} = 0.9\sqrt{2g_0 \Delta H} = 297.52\frac{m}{s}$$

Supposing the inlet velocity $v_1 = 15\ m/s$, we find $A_1 = Q/v_1 = 0.0277\ m^2$. The pump inlet flow needs to be increased by the shaft cross section area of the shaft $A_{shaft} = 0.125\ m^2 (D_{shaft} = 0.4\ m)$. Finally we can obtain the initial diameters of the impeller

$$D_1 = \sqrt{\frac{4(A_1 + A_{shaft})}{\pi}} = 0.44\ m$$

This is enough information to draw a preliminary sketch of the impeller of the ox pump.

6.4.3. Turbine

The turbine is responsible for generating sufficient power to drive propellant pumps at the desired speeds and torques. It harnesses energy from the expansion of a gaseous working fluid through fixed nozzles and rotating turbine blades. These blades, attached to disks, are mounted on the turbine shaft. As the working gas expands through inclined nozzles, it acquires a high tangential velocity and then passes through specially shaped blades. Here, the gas's kinetic energy is converted into tangential forces on each blade, causing the turbine wheel to rotate.

According to an unofficial 3D model (Figure 6.8 e **Error! Reference source not found.**), SpaceX utilizes reaction turbines where the gas expansion is divided relatively evenly between rotating and stationary blade elements.

For the gas generator engine cycles, the design aims for high turbine efficiencies and elevated turbine inlet temperatures to minimize the flow of turbine working fluids. In gas generator cycles, it also seeks to increase the overall effective specific impulse and thus reduce the propellant mass required

to drive the turbine. However, factors such as reliability, gas temperature variations, and cost considerations, particularly when using special steel alloys for blade and disk materials, have led to more conservative turbine inlet temperatures of approximately 900 to 950 K, as we have set in the calculation of the cycle.

With well-designed turbines and robust high-temperature materials, maximum blade speeds typically range from 400 to 700 m/sec. Higher blade speeds generally result in improved efficiencies.

6.4.4. Other Consideration

From unofficial CAD designs, we can see the complexity of this system, which plays a crucial role in the success of the engine itself. The entire system underwent thorough dynamic studies, with special attention given to manufacturing. The choice of materials is essential to withstand the stresses and temperatures involved. In a deeper study and development, it is necessary to analyse the start up transient of the turbopump system. Based on information and schematics found online, it seems that the start up relies on a subsystem of helium or nitrogen injected directly into the turbine through a spin-up volute (see CAD). The turbopump system must be able to regulate the engine and operate at different speeds. It is also crucial to control and study the vibrations caused by the rotation of the shaft and the enormous energy generated by the engines. Avoiding resonance frequencies becomes vital to prevent engine failure or even spacecraft loss.

In conclusion, we have the CAD models published by @hisdirtremoves on Twitter, which attempt to recreate the turbopump system used by SpaceX.
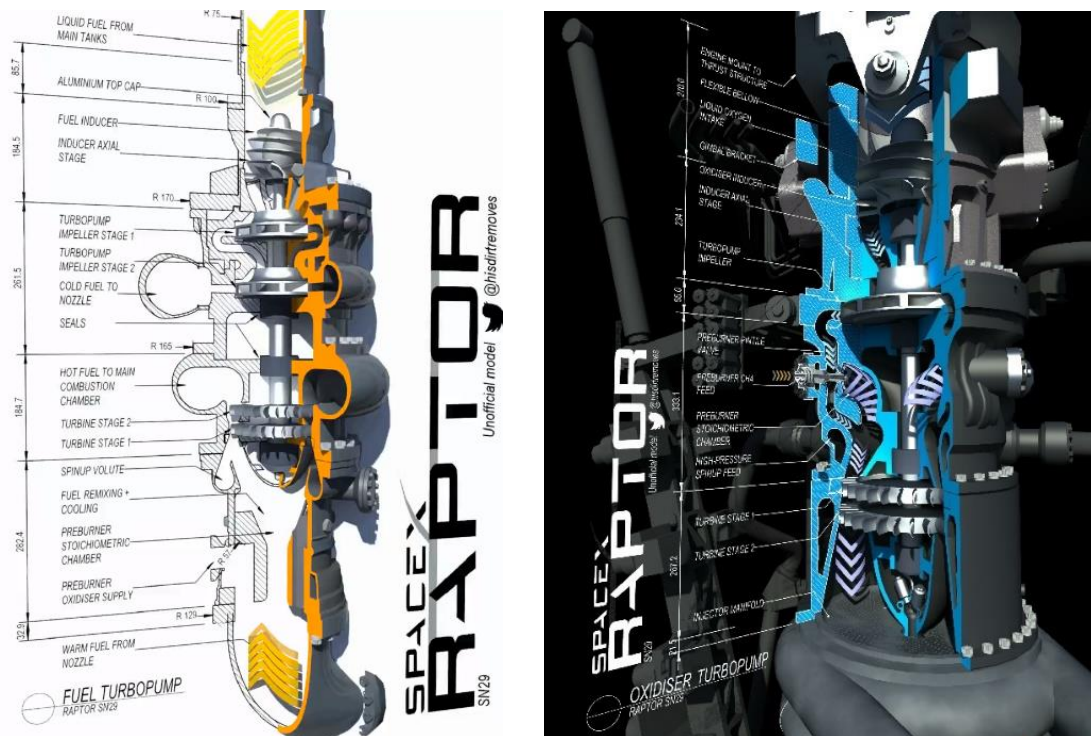

Figure 6.8: OX Turbopump CAD (Left) and CH4 Turbopump CAD (Right)

6.5. Cooling Jacket

6.5.1. Introduction and Method

Cooling is used in order to prevent chambers and nozzle walls from failing due to high temperatures. The steady-state method and transient or unsteady heat transfer method are two cooling methods presently in common use. The second one is mostly applied with low chamber pressures and low heat transfer rates. The first one includes regenerative cooling and radiation cooling. Regenerative cooling enables to reach greater pressures and high heat transfer rates. Indeed, this method is the one used on the Raptor engine. It is done with cooling jackets built around the thrust chamber where one liquid propellant circulates through before it is fed to the preburner. The fluid coolant is methane; indeed, fuels are usually used to cool in this situation.

6.5.2. Design and Cycle configuration

Since the actual design configuration of the Raptor's cooling jacket is unknown, we decided to suppose a milled channel design to dimension the system. This is because it is the one that usually can accept the highest heat transfer intensities. It consists of rectangular cooling channels of varying width and depth and a relatively thick contoured inner wall using a high conductivity material.

Figure 6.9: Milled channel design

The wall material is SX500, a monocrystal nickel alloy, oxidation-corrosion-resistant material well suited for service in extreme environments subjected to pressure and heat. A fraction of methane flows from the turbopump to the cooling channels. The cooling starts from the throat region, where the heat transfer is the highest. After cooling the thrust chamber, it flows to the methane preburner as it is shown by the following scheme.
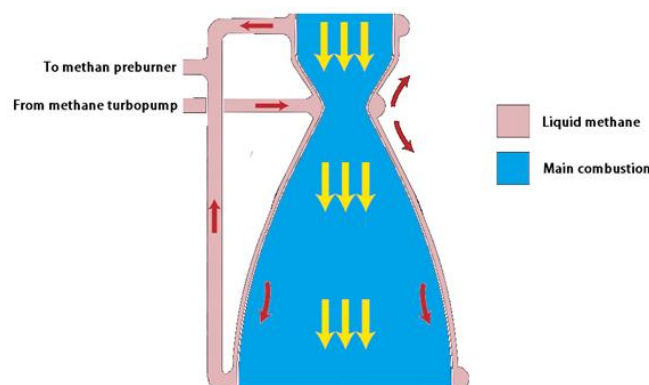

Figure 6.10: Cooling cycle

6.5.3. Sizing Model

The sizing model is illustrated in the MatLab file "RaptorCoolingJacket". The dimensioning goal is to define the right thickness of the thrust chamber wall (t_w) and the coolant temperature curve along the combustion chamber. The inputs are the following methane properties:

- Inlet temperature T_{in}
- Mass flow rate $\dot{m}$
- Specific heat transfer c
- Density ρ
- Dynamic viscosity μ

The other inputs are:

- Thrust chamber length
- SX500 thermal conductivity k
- Number of ducts n_c
- Wall gas temperature T_{wg}
- Pressure drop coefficient ΔP

At the outlet the methane remains still liquid. Therefore, the outlet temperature must be lower than the boiling temperature of methane at that given pressure. The latter can be calculated using the Clausius Clapeyron law:

$$T_{out} = \frac{1}{(\frac{1}{T_{ref}} - \ln\left(\frac{P_{out}}{P_{ref}}\right) \cdot \frac{R}{\Delta H})}$$

Where ΔH is the enthalpy of vaporization at a reference temperature T_{ref} and pressure P_{ref} equal to ambient pressure, R the universal gas constant, P_{out} the outlet pressure. P_{out} is obtained from P_{in} multiplied by the pressure drop coefficient. In order to avoid transients in which the methane can become gas, it was decided to size the system considering the achievement of 70% of the temperature given by the latter law.

From this data the programme runs two cycles to determine the requested outputs. One is the cycle from the throat to the top of the thrust chamber and the other one to the bottom. Both cycles are based on these equations:

$$\dot{m} = \frac{q \cdot A}{c * (T_{l+1} - T_l)} \qquad q = \frac{(T_{wg} - T_l)}{(\frac{t_w}{k} + \frac{1}{h_l})} \qquad h_l = 0.023 c \dot{m} A_d \left(\frac{d_d v \rho}{\mu}\right)^{-0.2} - 0.2\left(\frac{\mu c}{\kappa}\right)^{-\frac{2}{3}}$$

Where q is the heat flux, A the thrust chamber side area, T_l the coolant temperature, T_{l+1} the coolant temperature at the next nearest point, h_l the liquid-film coefficient, A_d the ducts area, d_d the ducts equivalent diameter, v the velocity of the coolant, κ the liquid-film conductivity. During the cycle the thrust chamber is divided in smaller sections to discretize the analysis of heat exchange. This allows to obtain local solutions. The diameter of the thrust chamber varies along the chamber and it is

interpolated from the data of chamber length and radius. After all the iterations the following geometry parameters are calculated:

- Circumference $C = \pi d$
- Effective circumference $C_{eff} = C - t_{sw} \cdot n_c$ (t_{sw} is the thickness of the duct side wall and was supposed equal to that of the thrust chamber wall)
- Heat exchange area $A_h = C_{eff} \cdot h$
- Duct width $w_d = \frac{C_{eff}}{n_c}$
- Duct height $h_d = \frac{w_d}{2}$
- Duct area $A_d = C_{eff} \cdot h$
- Hydraulic diameter $d_d = \frac{4A_d}{2(w_d + h_d)}$

Then the local coolant temperature is obtained from the equations above of mass flow and heat flux. The cycle ends when the difference between the obtained outlet temperature and the requested one is less than a fixed tolerance of 0.1 K. The respective wall thickness values obtained are 0.879 mm for the lower part and 0.334 mm for the upper part.

6.5.4. Temperature Curve

The following temperature trend denotes an almost linear variation trend considering the two parts in which the cooling cycle is divided, starting from the chamber throat with a temperature of 142.72 K and ending with a final temperature of 288.20 K.
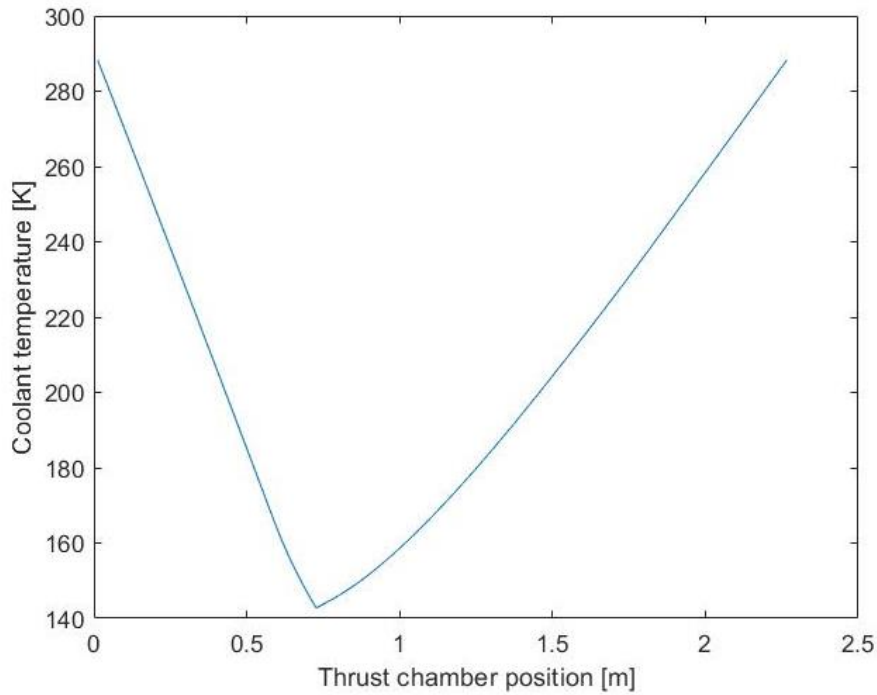
Graph 6.3: Temperature curve in cooling jacket

6.6. Injector

6.6.1. Injector Type

From a YouTube's video where Elon Musk speaks about the Raptor we have understood that the injectors used inside the Raptor 2 follow the template of swirl injectors. The oxidizer rich feed enters vertically into the chamber of a single injector while the fuel rich feed enters horizontally, perpendicular to the other one. So, the fluid begins to rotate inside the hollow. The mixing happens inside the injector chamber caused by the turbulent movement of the flowing. When the mixed fluid reaches the orifices, it exits with the shape of a cone made of droplets.
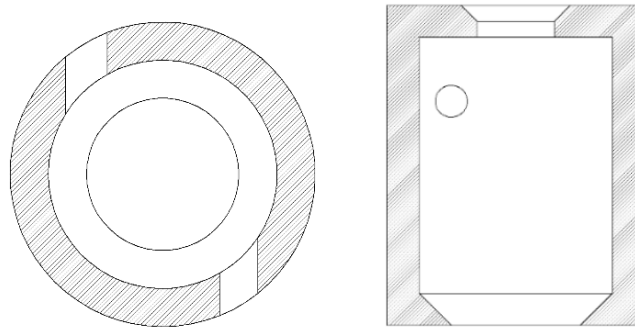
Figure 6.11: Injector type

Since the sources do not explain this, we have supposed that the orifices between the injector chamber and the combustion chamber are short tube with spiral effect. These orifices have a cone entrance that is going to increase the tangential velocity, which permits better atomization. Instead, the orifices between the inlet feed of the oxidizer rich fluid and the injector chamber are short tube with conical entrance, while the orifices between the inlet feed of the fuel rich fluid and the injector chamber are short tube with rounded entrance.

Figure 6.12: Short tube with spiral effect

Figure 6.13: Short tube with conical entrance

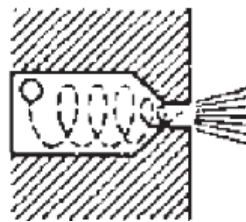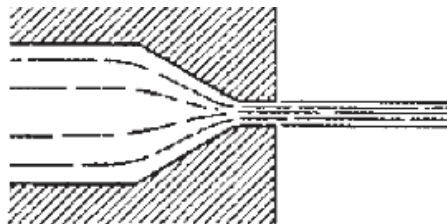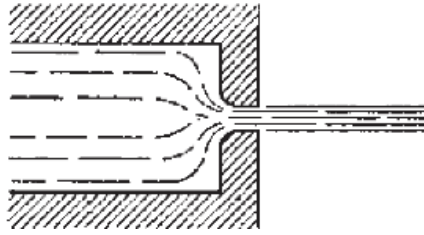Figure 6.14: Short tube with rounded entrance

The atomization happens inside the combustion chamber using the tangential velocity of the mixed fluid. When the flowing goes out of the injector, it is reduced to droplets allocated on a simple spray. This allows the combustion to be efficient. As the fluid goes more rapidly, the cone will get bigger.

6.6.2. Sizing of the injector

The dimensioning of the injector has been done using different hypotheses:

  o C_{d_I} between the injector chamber and the combustion chamber is 0.45;
  o C_{d_F} between the Fuel Rich feed and the injector chamber is 0.9;
  o C_{d_O} between the Oxidizer Rich feed and the injector chamber is 0.8;
  o   the pressure drop between the combustion chamber and the injector chamber is 10% of the pressure inside the combustion chamber: $\Delta P_1 = 0.1 \cdot P_C = 30\ bar$;
  o   the pressure drop between the injector chamber and the inlet feed is 10% of the pressure inside the injector chamber: $P_I = P_C + \Delta P_1 = 330\ bar$, $\Delta P_2 = 0.1 \cdot P_I = 33\ bar$;
  o   the orifice diameter of a single injector is 4 mm, $D_{1H} = 0.004\ m$;
  o   the ratio between the number of holes for fuel and the number of holes for oxidizer is 2:1 (F:O);
  o   mixing complete, that allows to calculate the density of the mixed fluid with this equation, $\rho_{MIX} = \frac{\frac{O}{F} \cdot \rho_{O} + \rho_F}{1 + \frac{O}{F}}$. In truth, the mixing is not completed in the injector chamber but will be completed in the combustion chamber, with the intersection of the spray with the other sprays of the other injectors.

Now, going through the difficult, we calculate the area of a single hole of the exit:

$$A_{1H_I} = \frac{\pi D_{1H}^2}{4} = 1.2566 \cdot 10^{-5}\ m^2$$

Then, using the equation of the discharge coefficient $C_d = \frac{\dot{m}}{A_H \sqrt{2\rho\Delta P}}$, we can obtain the area needed for all the flow rate of the rocket:

$$A_{H_I} = \frac{\dot{m}_p}{C_{d_I} \sqrt{2\rho_{MIX}\Delta P_1}} = 0.03717\ m^2$$

After this, we can estimate the number of injectors required for this case, dividing the area needed for all the flow rate by the area of a single hole:

$$N_I = \frac{A_{H_I}}{A_{1H_I}} = 2959$$

Afterward, we can compute the flow rate of a single injector, dividing the total flow rate by the number of injectors, and, using the mixing ratio, also the flow rate of Fuel Rich and the flow rate of Oxidizer Rich:

$$\dot{m}_{1I} = \frac{\dot{m}_{tot}}{N_I} = 0.2304 \ \frac{kg}{s} \qquad \dot{m}_{1F} = \frac{\dot{m}_I}{1+\frac{O}{F}} = 0.0524 \ \frac{kg}{s} \qquad \dot{m}_{1O} = \dot{m}_p - \dot{m}_{1F} = 0.1781 \ \frac{kg}{s}$$

Using these flow rates, we can obtain the area and diameter of the holes for the Fuel Rich feed inlet and the Oxidizer Rich feed inlet:

$$A_{1H_F} = \frac{\dot{m}_{1F}}{2 \cdot C_{d_F}\sqrt{2\rho_F \Delta P_2}} = 1.3371 \cdot 10^{-6} \ m^2 \qquad D_{1H_F} = \sqrt{\frac{4 \cdot A_{1H_F}}{\pi}} = 0.0013 \ m$$

$$A_{1H_O} = \frac{\dot{m}_{1O}}{C_{d_O}\sqrt{2\rho_O \Delta P_2}} = 6.8907 \cdot 10^{-6} \ m^2 \qquad D_{1H_O} = \sqrt{\frac{4 \cdot A_{1H_O}}{\pi}} = 0.0030 \ m$$

So, the injector will be like this:
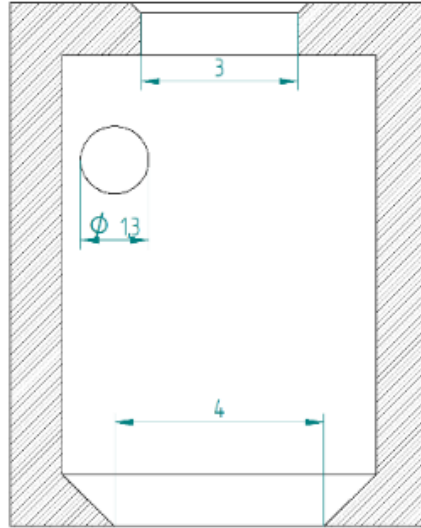
Figure 6.15: Injector Geometry

Moreover, we can calculate the velocity of both fluid:

$$u_F = C_{d_F}\sqrt{\frac{2 \cdot \Delta P_2}{\rho_F}} = 136.4814 \ \frac{m}{s} \qquad u_O = C_{d_O}\sqrt{\frac{2 \cdot \Delta P_2}{\rho_O}} = 81.7258 \ \frac{m}{s}$$

$$u_{MIX} = C_{d_I}\sqrt{\frac{2 \cdot \Delta P_1}{\rho_{MIX}}} = 66.2341 \ \frac{m}{s}$$

It permits us to estimate the dynamic pressure drop inside the injectors:

$$\Delta P_{dyn_F} = \frac{1}{2}\rho_F u_F^2 = 13.3650 \ bar \qquad \Delta P_{dyn_O} = \frac{1}{2}\rho_O u_O^2 = 10.5600 \ bar$$

$$\Delta P_{dyn_{MIX}} = \frac{1}{2}\rho_{MIX} u_{MIX}^2 = 6.0750 \ bar$$

7 Conclusion

In this final chapter, we will compare the Raptor engine with other engines to see how effective and important this project is. We'll also compare the two versions of the engine, talking about the main differences and what's coming next.

7.1. Comparing Raptor and other space engine

	Merlin	RD-180	F-1	Raptor	BE-4	RS-25
Cycle	Open	Closed (LOX rich)	Open	Closed (Full Flow)	Closed (LOX rich)	Closed (Fuel Rich)
Fuel Type	RP-1	RP-1	RP-1	Methane	Methane	Hydrogen
Total Thrust	0.84 MN	3.83 MN	**6.77 MN**	2.00 MN	~2.40 MN	1.86 MN
Thrust : Weight	**198 : 1**	78 : 1	94 : 1	107 : 1	~80 : 1	73 : 1
Specific Impulse (ISP)	282 sl / 311 vac	311 sl / 338 vac	263 sl / 304 vac	330 sl / ~350 vac	~310 sl / ~340 vac	**366 sl / 452 vac**
Chamber Pressure	97 bar	257 bar	70 bar	**270 bar**	~135 bar	206 bar

Figure 7.1: Raptor vs other space engine

In this image we see the comparison between some engines: we have SpaceX's open cycle Merlin engine that powers Falcon 9 and Falcon 9 Heavy rockets, the oxygen-rich closed cycle RD-180 that powers Atlas V rocket, the open cycle F-1 engine which powered Saturn V, then there is the Raptor that powers Starship and Super Heavy booster, then we have the closed cycle oxygen rich BE-4 engine that uses methane as fuel that will power New Glenn rocket and Vulcan rocket and last but not least the closed cycle fuel rich RS-25 engine that powered the Space Shuttle and will power the SLS rocket which runs on hydrogen. Analyzing every comparable aspect of these engines we start with the total thrust from the lowest to the highest: the Merlin produces 0.84 MNs of thrust, the RS-25 produces 1.86 MNs, the Raptor is around 2 MNs, the BE-4(in development) is hoping to hit 2.4 MNs, the RD-180 // 3.83 MNs and the F-1 is still the best with 6.77 MNs. Then we have the thrust to weight ratio which tells us how heavy the engine is compared to how much thrust it produces; here the lowest is the Space Shuttle's RS-25 at 73:1, then there's the RD-180 which is 78:1, then we have the BE-4 at around 80:1 (approximate data), then we have the F-1 is 94:1, then we have the Raptor at 107:1 (for now), and lastly the Merlin is the leader with his 198:1 thrust to weight ratio. Our analysis continues talking about the specific impulse measured in seconds. So starting with the least efficient engine which is the F-1 engine at 263 to 304 seconds, then the Merlin engine at 282 to 311 seconds, then we get the RD-180 at 311 to 338 seconds and the BE-4 which is around 310 to 340 seconds, next up is the Raptor engine which is 330 to around 350 seconds, and lastly the king here by far is the RS-25 which

is 366 to 452 seconds! The last aspect that we are going to compare is the chamber pressure which affects both thrust and specific impulse. Generally, the higher the chamber pressure, the more thrust and potentially more efficiency the engine can gain. Working with high chamber pressures allows the engine to be smaller for a given thrust level and, doing this, it improves the thrust to weight ratio. Here we have the F-1 which only had 70 bar in its chamber pressure. So next up is the Merlin engine at 97 bar, then the BE-4 will be around 135 bar, then the RS-25 which is 206 bar, then the RD-180 which was the king of operational engines at 257 bar before the Raptor which is the best talking about chamber pressure with 270 bars c.a. looking forward to overcome the 300 bars barrier.

Is the Raptor engine really the king of rocket engines? Well, rocket science, like all things is a complex series of compromises. Is it the most efficient engine, no. Is it the most powerful engine, no. Is it the cheapest engine, probably not. Is it the most reusable engine, maybe. But does it do everything really well? YES. It truly is a goldilocks engine, doing everything it needs to do very well. It is the perfect fit for your interplanetary spaceship.

7.2.   Comparing the Evolution of the Raptor Engine

In a brief summary, it may initially seem that the Raptor 2 is incomplete compared to the first version, but this is not the case. Let's quickly review all the changes made by Musk, as analyzed earlier.
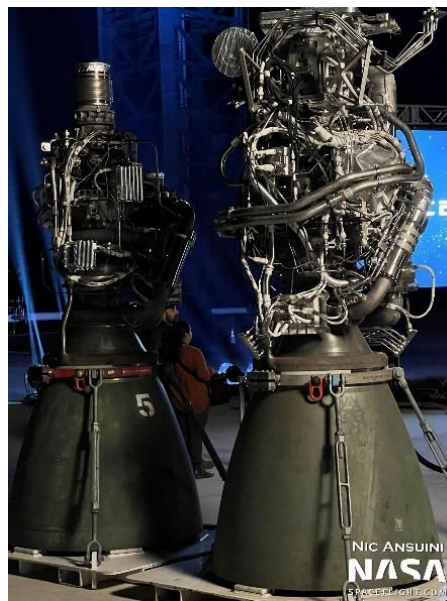
Figure 7.2: Raptor 2 (Left) and Raptor 1 (Right)

Firstly, the aesthetic appearance is different, with many tubes, wires, and thermal protections removed to reduce weight. The use of methane and oxygen as fuel and oxidizer, respectively, allowed the elimination of igniters in the combustion chamber. These igniters are still present in the preburner, but not in the combustion chamber itself. The two reactants enter the chamber as extremely hot gases, resulting in clean and well-mixed interactions.

The combustion chamber pressure has been increased, allowing for a thrust of 230 tons compared to the 185 tons of the Raptor 1. However, the most important change is the increase in throat area (as we can see in the chapter 3). This allows for a greater propellant flow, and consequently, a higher thrust. The downside is the reduction in the expansion ratio, which is essential in a rocket engine as it represents the work and efficiency of the nozzle. Sometimes, accepting compromises in certain areas can lead to greater overall benefits.

Despite all these modifications, Musk intends to make many more, considering the Raptor still at the beginning of its maximum development. So, what can we expect?

Certainly, further efforts will be made to streamline the engine to reduce weight and production costs. Additionally, there are attempts to remove throat film cooling.

In May 2023, SpaceX started testing the version 3 of its rocket, as stated by Elon Musk. On Twitter, he congratulated SpaceX and shared a graph of a static fire with a 350 bar chamber pressure and a thrust of 269 tons (approximately 17% higher). This development indicates SpaceX's continuous efforts to improve their rocket technology for future space missions.

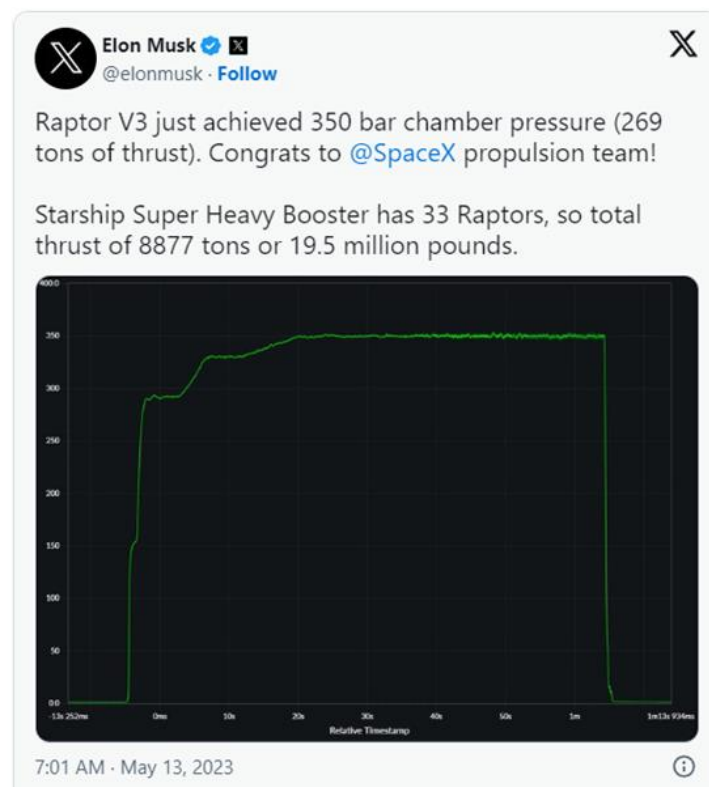Figure 7.3: Tweet by Elon Musk announcing version 3 of the Raptor engine

In conclusion, the Raptor 2 engine by SpaceX is one of the most exciting projects under development. It incorporates cutting-edge technologies and engineering solutions aimed at reducing costs and production time. The Raptor engine could be the one that lands humans on the Moon and takes us to Mars.

List of Figures

List of Tables

List of Graphs

Code

Here are the MATLAB codes that have been utilized to determine the numerical values of this report.

RaptorCycleAnalysis.m

```matlab
1    clear all
2    clc
3
4    % parametre of the cycle
5    TOLL = 1;
6    PREC = 3;
7
8    %%%%%% Initial Data %%%%%%%
9
10   % Data of preburner fuel-rich
11   T_PREB_RCH4 = 950;
12   fo_preburner_rch4 = 1/0.22;
13
14   % Data of preburner ox-rich
15   T_PREB_ROX = 770;
16   of_preburner_rox = 50;
17
18   % Data of main chamber
19   m_flow_nozzle = 681.89; % kg/s
20   p_main_chamber = 300; % bar
21   of_main_chamber = 3.4;
22
23   % efficiency
24   eta_turbina_ox = 0.72;
25   eta_pump_ox = 0.75;
26   eta_pump_ch4 = 0.7;
27   eta_turbina_ch4 = 0.65;
28   eta_mec = 0.98;
29   beta_preburner = 0.95;
30
31   % pressure drop
32   p_lost_beta_cooling = 0.35*p_main_chamber;
33   p_lost_valve = 0.05*p_main_chamber;
34   %p_lost_injector = 0.8*(p_main_chamber)^0.5;
35   p_lost_injector = 46;
36
37   % tank OX
38   T_ox_0 = 63; %K
39   p_ox_0 = 4; % kPa
40
41   % thermodynamics property
42   [H_ox_0, S_ox_0, rho_ox_0] = refpropm('HSD','T', T_ox_0,'P',p_ox_0*100,'oxygen');
43
44   % tank CH4
45   T_ch4_30 = 97; %K
46   p_ch4_30 = 4; % kPa
47
48   % thermodynamics property
49   [H_ch4_30, S_ch4_30, rho_ch4_30]  = refpropm('HSD','T', T_ch4_30,'P',p_ch4_30*100,'methane');
50
```

```matlab
51    % vector/matrix of result
52    p_rox_14 = [];
53    p_ox_14_vector = [];
54    t_preburner_rox = [];
55    t_preburner_rch4 = [];
56    power_pump_ox = [];
57    power_pump_ch4 = [];
58
59    % Mass Balance
60    m_ch4 = m_flow_nozzle/(of_main_chamber + 1);
61    m_ox = m_flow_nozzle - m_ch4;
62
63    m_ch4_supply = (m_ox - 1/fo_preburner_rch4*m_ch4)/(of_preburner_rox -
1/fo_preburner_rch4);
64    m_ch4_main = m_ch4 - m_ch4_supply;
65
66    m_ox_supply = (m_ch4 - m_ch4_supply)/fo_preburner_rch4;
67    m_ox_main = m_ox - m_ox_supply;
68
69    m_rch4 = m_ox_supply + m_ch4_main;
70    m_rox =  m_ch4_supply + m_ox_main;
71
72    % starting guess
73    start_pump_ox = 640;
74    start_pump_ch4 = 750;
75    p_ox_2 = start_pump_ox;
76    p_ch4_32 = start_pump_ch4;
77
78    %% Calculation
79    while 1
80        % ----- OX ------
81        % pipes 1 ox
82        m_ox_17 = m_ox;
83        p_ox_1 = p_ox_0;
84
85        % Pump 2 ox
86        H_ox_2_ideal = refpropm('H','P',p_ox_2*100,'S', S_ox_0,'oxygen');
87        H_ox_2_real = H_ox_0 + (H_ox_2_ideal - H_ox_0)/eta_pump_ox;
88        [T_ox_2, S_ox_2, rho_ox_2] = refpropm('TSD', 'P', p_ox_2*100, 'H', H_ox_2_real,
'oxygen');
89
90        % lost pressure between pump and preburner
91
92        % pipes 3 ox
93        m_ox_3 = m_ox;
94        p_ox_3 = p_ox_2;
95
96        % valve of regulation 4 ox main
97        m_ox_4 = m_ox_main;
98        p_ox_4 = p_ox_3 - p_lost_valve;
99
100       % valve of regulation 5 ox supply
101       m_ox_5 = m_ox_supply;
102       p_ox_5 = p_ox_3 - p_lost_valve;
103
104       % pipes 6 ox main
105       m_ox_6 = m_ox_4;
106       p_ox_6 = p_ox_4;
107
108       % pipes 15 ox supply
109       m_ox_15 = m_ox_5;
110       p_ox_15 = p_ox_5;
111
112       % injector ox supply
113       m_ox_17 = m_ox_15;
114       p_ox_17 = p_ox_15 - p_lost_injector;
115
```

```matlab
116         % ----- CH4 -------
117         p_rch4_45 = [];
118         power_pump_ch4 = [];
119         p_ch4_45_vector = [];
120         t_preburner_rch4 = [];
121         p_ch4_32 = start_pump_ch4;
122
123         % pipe 31
124         m_ch4_31 = m_ch4;
125         p_ch4_31 = p_ch4_30;
126
127         while 1
128             % Pump ch4 32
129             H_ch4_32_ideal = refpropm('H','P',p_ch4_32*100,'S', S_ch4_30,'methane');
130             H_ch4_32_real = H_ch4_30 + (H_ch4_32_ideal - H_ch4_30)/eta_pump_ch4;
131             [T_ch4_32, S_ch4_32, cp_ch4_32, rho_ch4, viscostita_dinamica_ch4] =
refpropm('TSCDV', 'P', p_ch4_32*100, 'H', H_ch4_32_real, 'methane');
132             m_ch4_32 = m_ch4_31;
133             power_pump_ch4_bis = m_ch4 * (H_ch4_32_real-H_ch4_30);
134
135             % pipes 33
136             p_ch4_33 = p_ch4_32;
137             m_ch4_33 = m_ch4_32;
138
139             % cooling jacket 34
140             p_ch4_34 = p_ch4_33 - p_lost_beta_cooling;
141             m_ch4_34 = m_ch4_33;
142
143             % pipes 35 ch4
144             p_ch4_35 = p_ch4_34;
145             m_ch4_35 = m_ch4_34;
146             S_ch4_35 = refpropm('S','T', 288,'P', p_ch4_35*100,'methane');
147
148             % valve of regulation 46 (supply)
149             p_ch4_46 = p_ch4_35 - p_lost_valve;
150             m_ch4_46 = m_ch4_supply;
151
152             % pipes 47 ch4 (supply)
153             p_ch4_47 = p_ch4_46;
154             m_ch4_47 = m_ch4_46;
155
156             % valve of regulation  pressure 48 (supply)
157             p_ch4_48 = p_ox_6;
158             p_lost_48 = p_ch4_47-p_ox_6;
159             m_ch4_48 = m_ch4_47;
160
161             % injector 49 ch4 (supply)
162             p_ch4_49 = p_ch4_48 - p_lost_injector;
163             m_ch4_49 = m_ch4_48;
164
165             % valve of regulation 36 main
166             p_ch4_36 = p_ch4_35- p_lost_valve;
167             m_ch4_36 = m_ch4_main;
168
169             % pipes 37 ch4 main
170             p_ch4_37 = p_ch4_36;
171             m_ch4_37 = m_ch4_36;
172
173             % valve of regulation  pressure 38 (main)
174             p_ch4_38 = p_ch4_37;
175             p_lost_38 = p_ch4_37 - p_ox_15;
176             m_ch4_38 = m_ch4_37;
177
178             % injector preburner 39
179             m_ch4_39 = m_ch4_38;
180             p_ch4_39 = p_ch4_38 - p_lost_injector;
181
```

```matlab
182             % preburner 40
183             p_rch4_preburner = p_ch4_39;
184             [h_ch4_main, t_ch4_main] = refpropm('HT','P', p_ch4_39*100,'S',
    S_ch4_35,'methane');
185             [h_ox_supply, t_ox_supply] = refpropm('HT','P', p_ch4_39*100,'S',
    S_ox_2,'oxygen');
186             RCH4 = CEA('problem', 'tp', 'o/f', 1/fo_preburner_rch4 , 'p,bar',
    p_rch4_preburner, 't,k', T_PREB_RCH4, 'case', 'PreBurner CH4 RICH', 'reac', 'fu', 'CH4(L)',
    'C', 1,'H', 4, 'h,j/kg',h_ch4_main, 't,k', t_ch4_main,'ox', 'O2(L)', 'O', 2,
    'h,j/kg',h_ox_supply, 't(k)', t_ox_supply,  'output', 'tran', 'massf', 'end');
187             cp_rch4 = RCH4.output.cp;
188             gamma_rch4 = RCH4.output.gamma;
189             t_preburner_rch4 = [t_preburner_rch4 RCH4.output.temperature];
190
191             % gas duct ch4 e preburner out 41
192             T_rch4_41 = RCH4.output.temperature;
193             p_rch4_41 = p_rch4_preburner*beta_preburner;
194
195             % turbine ch4 gas ideale 42
196             T_rch4_42 = (eta_mec^2*m_rch4*cp_rch4*1000*T_rch4_41 - m_ch4*(H_ch4_32_real -
    H_ch4_30))/(eta_mec^2*m_rch4*cp_rch4*1000);
197             T_rch4_42_ideal = T_rch4_41 - (T_rch4_41 - T_rch4_42)/eta_turbina_ch4;
198             power_pump_ch4 = [power_pump_ch4, eta_mec^2*m_rch4*cp_rch4*1000*(T_rch4_41 -
    T_rch4_42)];
199
200
201             p_rch4_42 = p_rch4_41*(T_rch4_42_ideal/T_rch4_41)^(gamma_rch4/(gamma_rch4 - 1));
202
203             %gas duct 43 ch4
204             p_rch4_43 = p_rch4_42;
205             m_rch4_43 = m_rch4;
206
207             % valve of regulation  pressure 44 (supply)
208
209             %injector 45 ch4
210             p_rch4_45 = [p_rch4_45 p_rch4_43-p_lost_injector];
211             p_ch4_45_vector = [p_ch4_45_vector, p_ch4_32];
212             if (abs(p_rch4_45(end) - p_main_chamber) < TOLL)
213                 break;
214             else
215                 if(p_rch4_45(end) < p_main_chamber)
216                     p_ch4_32 = p_ch4_32 + PREC;
217                 else
218                     p_ch4_32 = p_ch4_32 - PREC;
219                 end
220             end
221         end
222         % ------ OX ----------
223
224         % injector preburner 8 ox main
225         m_ox_8 = m_ox_6;
226         p_ox_8 = p_ch4_48 - p_lost_injector;
227
228         % preburner 9 ox
229         p_rox_preburner = p_ch4_49;
230         [h_ch4_supply, t_ch4_supply] = refpropm('HT','P', p_rox_preburner*100,'S',
    S_ch4_32,'methane');
231         [h_ox_main, t_ox_main] = refpropm('HT','P', p_rox_preburner*100,'S',
    S_ox_2,'oxygen');
232         ROX = CEA('problem', 'tp', 'o/f', of_preburner_rox,'t,k', T_PREB_ROX,'p,bar',
    p_rox_preburner, 'case', 'PreBurner OX RICH', 'reac', 'fu', 'CH4(L)', 'C', 1,'H', 4,
    'h,j/kg',h_ch4_supply, 't,k', t_ch4_supply,'ox', 'O2(L)', 'O', 2, 'h,j/kg',h_ox_main, 't,k',
    t_ox_main, 'output', 'tran', 'massf', 'end');
233
234         cp_rox = ROX.output.cp;
235         t_preburner_rox = [t_preburner_rox ROX.output.temperature];
236         gamma_rox = ROX.output.gamma;
237
```

```matlab
238            % gas duct 10 ox
239            m_rox_10 = m_rox;
240            T_rox_10 = ROX.output.temperature;
241            p_rox_10 = p_rox_preburner*beta_preburner;
242
243            % turbine ox gas ideale ox 11
244            T_rox_11 = (eta_mec^2*m_rox*cp_rox*1000*T_rox_10 - m_ox*(H_ox_2_real -
       H_ox_0))/(eta_mec^2*m_rox*cp_rox*1000);
245            T_rox_11_ideal = T_rox_10 - (T_rox_10 - T_rox_11)/eta_turbina_ox;
246            power_pump_ox = [power_pump_ox, eta_mec^2*m_rox*cp_rox*1000*(T_rox_10 - T_rox_11)];
247
248            p_rox_11 = p_rox_10*(T_rox_11_ideal/T_rox_10)^(gamma_rox/(gamma_rox - 1));
249
250            %gas duct 12 ox
251            p_rox_12 = p_rox_11;
252
253            %injector 14 ox
254            p_rox_14 = [p_rox_14 p_rox_12-p_lost_injector];
255            p_ox_14_vector = [p_ox_14_vector, p_ox_2];
256
257            if (abs(p_rox_14(end) - p_main_chamber) < TOLL)
258                break;
259            else
260                if(p_rox_14(end) < p_main_chamber)
261                    p_ox_2 = p_ox_2 + PREC;
262                else
263                    p_ox_2 = p_ox_2 - PREC;
264                end
265            end
266    end
267
268    %% figure pressure main-start pressure
269    close all
270    figure;
271
272    p_ox = plot(p_ox_14_vector, p_rox_14, '-ob');
273    target = yline(300, '--g');
274    hold on;
275
276    p_ch4 = plot(p_ch4_45_vector, p_rch4_45, '-or');
277    xlabel('Pumping pressure [bar]', 'FontSize', 15)
278    ylabel('Main Combustion chamber pressure [bar]', 'FontSize', 15)
279    legend([p_ox p_ch4 target], 'Rich Ox', 'Rich CH4', 'Target 300 bar', 'FontSize', 15)
280    title('Pressure in the combustion chamber as the pumping pressure varies','FontSize', 18)
281    %% figure power pump-start pressure
282    figure;
283    W_pump_ox = plot(p_ox_14_vector, power_pump_ox/10^6, '-ob');
284    target_ox = yline(37.97, '--b');
285    target_ch4 = yline(40.16, '--r');
286    hold on;
287    W_pump_ch4 = plot(p_ch4_45_vector, power_pump_ch4/10^6, '-or');
288    xlabel('Pumping pressure [bar]', 'FontSize', 15)
289    ylabel('Power [MW]', 'FontSize', 15)
290    legend([W_pump_ox W_pump_ch4 target_ox target_ch4], 'Ox', 'CH4', 'Target OX', 'Target
       CH4', 'FontSize', 15)
291    title('Required pump power as pumping pressure varies', 'FontSize', 18)
292
293    %%
294    of_final = m_rox*ROX.output.fractions(3)/m_rch4/RCH4.output.fractions(1);
295    mass_limit = m_rox*ROX.output.fractions(3) + m_rch4*RCH4.output.fractions(1);
296
297    CC = CEA('problem', 'rocket', 'fac', 'ma', m_flow_nozzle, 'supsonic(ae/at)', 34.34,'o/f',
       m_rox/m_rch4, 'p,bar', p_main_chamber,'reac', 'fu', 'Fuel_rich', 'C', 1,'H', 4, 'wtfrac',
       RCH4.output.fractions(1), 'H', 2, 'O', 1, 'wtfrac', RCH4.output.fractions(6), 'C', 1, 'wtfrac',
       RCH4.output.fractions(7),'h,kj/kg', RCH4.output.enthalpy, 't,k', T_rch4_42, 'rho, kg/m^3',
       RCH4.output.density, 'ox','Ox Rich', 'C',1,'O', 2, 'wtfrac', ROX.output.fractions(1),
       'H',2,'O', 1, 'wtfrac', ROX.output.fractions(2), 'O', 2, 'wtfrac',
       ROX.output.fractions(3),'h,kj/kg', ROX.output.enthalpy, 't,k', T_rox_11, 'rho,kg/m^3',
       ROX.output.density, 'output','transport','mks','end','screen');
```

RaptorTank.m

```matlab
1    clear all
2    close all
3    clc
4    %% Data
5    t_b = 300; % Burning Time
6    K_s = 1.05; % Security Coefficient
7    OF = 3.4; % Mixing Ratio
8    Qtot = 681.89; % Total Feed
9    rhoF = 443.27; % Methane Density
10   rhoO = 1269.18; % Oxygen Density
11   P_tank = 400000; % Tank Pressure (supposing)
12   T_tankF = 63; % Tank Temperature for Fuel (supposing)
13   T_tankO = 97; % Tank Temperature for Oxidizer (supposing)
14   Is = 327;
15   %% Feed
16   Q_F = Qtot/(1+OF); % Fuel Feed
17   Q_O = Qtot - Q_F; % Oxidizer Feed
18   %% Mass
19   M_F = Q_F*t_b*K_s; % Fuel Mass
20   M_O = Q_O*t_b*K_s; % Oxidizer Mass
21   %% Volume
22   V_F = M_F/rhoF; % Fuel Volume
23   V_O = M_O/rhoO; % Oxidizer Volume
24   %% Other Propulsive Parameters
25   rhoAV = (M_F + M_O)/(V_F + V_O); % Average Density
26   Iv = rhoAV*Is;% Volumertric Specific Impulse
27   Itot = Is*(M_F + M_O)*9.81;
28   %% Helium Data
29   THe_i = 290;
30   gammaHe = 1.66;
31   RHe = 2078.6;
32   %% Helium Pressurization for Fuel Tank
33   PHe_iF = P_tank*(THe_i/T_tankF)^(gammaHe/(gammaHe-1));
34   VHeF = [0];
35   MHeF = [0];
36   i = 1;
37   toll = 1;
38   while toll > 1e-5
39       i = i + 1;
40       MHeF(i) = (P_tank/(RHe*T_tankF))*(V_F + VHeF(i-1));
41       VHeF(i) = MHeF(i)/PHe_iF * THe_i*RHe;
42       toll = (MHeF(i) - MHeF(i-1))/MHeF(i);
43   end
44   %% Helium Pressurization for Oxidizer Tank
45   PHe_iO = P_tank*(THe_i/T_tankO)^(gammaHe/(gammaHe-1));
46   VHeO = [0];
47   MHeO = [0];
48   i = 1;
49   toll = 1;
50   while toll > 1e-5
51       i = i + 1;
52       MHeO(i) = (P_tank/(RHe*T_tankO))*(V_O + VHeO(i-1));
53       VHeO(i) = MHeO(i)/PHe_iO * THe_i*RHe;
54       toll = (MHeO(i) - MHeO(i-1))/MHeO(i);
55   end
```

RaptorCoolingJacket.m

```matlab
1     clear all
2     close all
3     clc
4
5     %% critical temperature
6     T1=111.63;%K
7     P1=1; %bar
8     Pin=835; %bar pressione in ingresso
9     cp=0.75; %pressure drop coefficient
10    P2=Pin*cp; %bar cooling jacket outlet pressure
11    DH=8.2e3; %J/mol
12    R=8.314; %J/K mol
13    T2=1/(1/T1-log(P2/P1)*R/DH); %critical temperature from the clausius clapeyron law
14
15    %% temperature and wall thickness along the combustion chamber
16    tw=0.1e-3; %m starting wall thickness for the cycle
17    c=3125.01; %J/kg°C specific heat transfer
18    T1=142.72; %inlet temperature
19    T2=T2*0.7; %outlet temperature
20    p=151.7826; %kg/s mass flow rate
21    kw=10; %W/mK SX500 thermal conductivity
22    kl=0.0339; %W/mK methane thermal conductivity
23
24    nc=100; %number of ducts
25    tol=0.1; %K temperature tolerance of the cycle
26    flag=1;
27    mu=1.35e-4;%Pa*s dynamic viscosity
28
29    %data is a matrix containing at every line the abscess along the chamber axis
30    %and the corrisponding temperature
31    data=[1.24275e-2; 3.70573e+3
32    3.87324e-2; 3.70573e+3
33    6.50373e-2; 3.70573e+3
34    9.13422e-2; 3.70573e+3
35    1.17647e-1; 3.70573e+3
36    1.43952e-1; 3.70573e+3
37    1.70257e-1; 3.70573e+3
38    1.96562e-1; 3.70573e+3
39    2.22867e-1; 3.70573e+3
40    2.49171e-1; 3.70573e+3
41    2.75476e-1; 3.70573e+3
42    3.01781e-1; 3.70573e+3
43    3.28086e-1; 3.70573e+3
44    3.54391e-1; 3.70573e+3
45    3.80696e-1; 3.70573e+3
46    4.07001e-1; 3.70573e+3
47    4.33306e-1; 3.70573e+3
48    4.59611e-1; 3.70573e+3
49    4.85915e-1; 3.70573e+3
50    5.12220e-1; 3.70658e+3
51    5.38525e-1; 3.71054e+3
52    5.64830e-1; 3.71421e+3
53    5.91135e-1; 3.71817e+3
54    6.17440e-1; 3.70799e+3
```

```
55      6.43745e-1; 3.66305e+3
56      6.66463e-1; 3.60157e+3
57      6.84398e-1; 3.53650e+3
58      6.99942e-1; 3.46788e+3
59      7.10485e-1; 3.39933e+3
60      7.19072e-1; 3.32796e+3
61      7.27442e-1; 3.25283e+3
62      7.31029e-1; 3.17665e+3
63      7.35812e-1; 3.10099e+3
64      7.39399e-1; 3.02668e+3
65      7.42986e-1; 2.94786e+3
66      7.47256e-1; 2.86269e+3
67      7.55284e-1; 2.76187e+3
68      7.63996e-1; 2.66815e+3
69      7.69505e-1; 2.60755e+3
70      7.90215e-1; 2.61699e+3
71      8.01574e-1; 2.57523e+3
72      8.27879e-1; 2.53893e+3
73      8.54184e-1; 2.48777e+3
74      8.80489e-1; 2.43378e+3
75      9.06794e-1; 2.38658e+3
76      9.33099e-1; 2.34305e+3
77      9.59403e-1; 2.30744e+3
78      9.85708e-1; 2.26504e+3
79      1.01201e+0; 2.22462e+3
80      1.03832e+0; 2.19183e+3
81      1.06462e+0; 2.16102e+3
82      1.09093e+0; 2.13219e+3
83      1.11723e+0; 2.10647e+3
84      1.14354e+0; 2.07820e+3
85      1.17012e+0; 2.03810e+3
86      1.19615e+0; 2.00669e+3
87      1.22177e+0; 1.99389e+3
88      1.24893e+0; 1.97390e+3
89      1.27611e+0; 1.95214e+3
90      1.30194e+0; 1.92949e+3
91      1.32701e+0; 1.91759e+3
92      1.35455e+0; 1.89706e+3
93      1.37983e+0; 1.88033e+3
94      1.40659e+0; 1.87091e+3
95      1.43334e+0; 1.85420e+3
96      1.45995e+0; 1.83399e+3
97      1.48550e+0; 1.81562e+3
98      1.51181e+0; 1.79965e+3
99      1.53799e+0; 1.78642e+3
100     1.56468e+0; 1.77457e+3
101     1.59162e+0; 1.76364e+3
102     1.61786e+0; 1.74755e+3
103     1.64333e+0; 1.73435e+3
104     1.66929e+0; 1.72309e+3
105     1.69594e+0; 1.71245e+3
106     1.72225e+0; 1.70326e+3
107     1.74747e+0; 1.69843e+3
108     1.77505e+0; 1.70444e+3
109     1.80116e+0; 1.70142e+3
110     1.82746e+0; 1.69351e+3
111     1.85377e+0; 1.68757e+3
112     1.88007e+0; 1.67853e+3
113     1.90638e+0; 1.67175e+3
114     1.93268e+0; 1.66355e+3
115     1.95899e+0; 1.65563e+3
116     1.98565e+0; 1.63469e+3
117     2.01160e+0; 1.62610e+3
```

```
118    2.03790e+0; 1.62073e+3
119    2.06421e+0; 1.61380e+3
120    2.09051e+0; 1.60583e+3
121    2.11682e+0; 1.60165e+3
122    2.14312e+0; 1.59656e+3
123    2.16943e+0; 1.59161e+3
124    2.19573e+0; 1.58497e+3
125    2.22204e+0; 1.57861e+3
126    2.24834e+0; 1.57253e+3
127    2.26628e+0; 1.56815e+3];
128
129    ndata=size(data,1);
130    lung=[];
131    Twg=[];
132
133    for i=1:ndata
134        if mod(i,2)==1
135            lung(end+1)=data(i); %abscess along the chamber axis
136        else
137            Twg(end+1)=data(i); %wall temperature in contact with gas
138        end
139    end
140    lung=lung';
141    Twg=Twg';
142
143    n=size(Twg,1);
144    Tl=zeros(n,1); %temperatura liquido
145
146    %raggiolung is a matrix containing at every line the abscess along the chamber axis
147    %and the corrisponding diameter
148    diamlung=[2.59187e-3; 1.63456e-1;
149    1.16963e-2; 1.64307e-1;
150    2.08008e-2; 1.64307e-1;
151    2.99052e-2; 1.64307e-1;
152    3.90097e-2; 1.64307e-1;
153    4.81141e-2; 1.64307e-1;
154    5.72185e-2; 1.64307e-1;
155    6.63230e-2; 1.64307e-1;
156    7.54274e-2; 1.64307e-1;
157    8.45319e-2; 1.64307e-1;
158    9.36363e-2; 1.64307e-1;
159    1.02741e-1; 1.64307e-1;
160    1.11845e-1; 1.64307e-1;
161    1.20950e-1; 1.64307e-1;
162    1.30054e-1; 1.64307e-1;
163    1.39159e-1; 1.64307e-1;
164    1.48263e-1; 1.64307e-1;
165    1.57367e-1; 1.64307e-1;
166    1.66472e-1; 1.64307e-1;
167    1.75576e-1; 1.64307e-1;
168    1.84681e-1; 1.64307e-1;
169    1.93785e-1; 1.64307e-1;
170    2.02890e-1; 1.64307e-1;
171    2.11994e-1; 1.64307e-1;
172    2.21099e-1; 1.64307e-1;
173    2.30203e-1; 1.64307e-1;
174    2.39307e-1; 1.64307e-1;
175    2.48412e-1; 1.64307e-1;
176    2.57516e-1; 1.64307e-1;
177    2.66621e-1; 1.64307e-1;
```

```
178    2.75725e-1; 1.64307e-1;
179    2.84830e-1; 1.64307e-1;
179    2.84830e-1; 1.64307e-1;
180    2.93934e-1; 1.64307e-1;
181    3.03039e-1; 1.64307e-1;
182    3.12143e-1; 1.64307e-1;
183    3.21247e-1; 1.64307e-1;
184    3.30352e-1; 1.64307e-1;
185    3.39456e-1; 1.64307e-1;
186    3.48561e-1; 1.64307e-1;
187    3.57665e-1; 1.64307e-1;
188    3.66770e-1; 1.64307e-1;
189    3.75874e-1; 1.64307e-1;
190    3.84979e-1; 1.64307e-1;
191    3.94083e-1; 1.64307e-1;
192    4.03187e-1; 1.64307e-1;
193    4.12292e-1; 1.64307e-1;
194    4.21396e-1; 1.64307e-1;
195    4.30501e-1; 1.64307e-1;
196    4.39605e-1; 1.64307e-1;
197    4.48710e-1; 1.64307e-1;
198    4.57814e-1; 1.64307e-1;
199    4.66919e-1; 1.64307e-1;
200    4.76023e-1; 1.64307e-1;
201    4.85128e-1; 1.64307e-1;
202    4.94232e-1; 1.64307e-1;
203    5.03336e-1; 1.64307e-1;
204    5.12441e-1; 1.64307e-1;
205    5.21545e-1; 1.64307e-1;
206    5.30650e-1; 1.64307e-1;
207    5.39754e-1; 1.64307e-1;
208    5.48859e-1; 1.64307e-1;
209    5.57963e-1; 1.64307e-1;
210    5.67068e-1; 1.64307e-1;
211    5.76172e-1; 1.64307e-1;
212    5.85276e-1; 1.64307e-1;
213    5.94381e-1; 1.63739e-1;
214    6.03485e-1; 1.61470e-1;
215    6.12590e-1; 1.58633e-1;
216    6.21694e-1; 1.53527e-1;
217    6.30799e-1; 1.48421e-1;
218    6.39903e-1; 1.43315e-1;
219    6.49008e-1; 1.38209e-1;
220    6.58112e-1; 1.34238e-1;
221    6.67216e-1; 1.30834e-1;
222    6.76321e-1; 1.27430e-1;
223    6.85425e-1; 1.25160e-1;
224    6.94530e-1; 1.23458e-1;
225    7.03634e-1; 1.21189e-1;
226    7.12739e-1; 1.21189e-1;
227    7.21843e-1; 1.19487e-1;
228    7.30948e-1; 1.19487e-1;
229    7.40052e-1; 1.21756e-1;
230    7.49156e-1; 1.25160e-1;
231    7.58261e-1; 1.30266e-1;
232    7.67365e-1; 1.35940e-1;
233    7.76470e-1; 1.41613e-1;
234    7.85574e-1; 1.47287e-1;
235    7.94679e-1; 1.52960e-1;
236    8.03783e-1; 1.58633e-1;
237    8.12888e-1; 1.64307e-1;
238    8.21992e-1; 1.69413e-1;
```

```
239    8.31096e-1; 1.74519e-1;
240    8.40201e-1; 1.80192e-1;
241    8.49305e-1; 1.85298e-1;
242    8.58410e-1; 1.90404e-1;
243    8.67514e-1; 1.96078e-1;
244    8.76619e-1; 2.00616e-1;
245    8.85723e-1; 2.06290e-1;
246    8.94828e-1; 2.11396e-1;
247    9.03932e-1; 2.16502e-1;
248    9.13036e-1; 2.21040e-1;
249    9.22141e-1; 2.26714e-1;
250    9.31245e-1; 2.31252e-1;
251    9.40350e-1; 2.36358e-1;
252    9.49454e-1; 2.41464e-1;
253    9.58559e-1; 2.46003e-1;
254    9.67663e-1; 2.50542e-1;
255    9.76768e-1; 2.55081e-1;
256    9.85872e-1; 2.60754e-1;
257    9.94976e-1; 2.65293e-1;
258    1.00408e+0; 2.69831e-1;
259    1.01319e+0; 2.74370e-1;
260    1.02229e+0; 2.78909e-1;
261    1.03139e+0; 2.83447e-1;
262    1.04050e+0; 2.87986e-1;
263    1.04960e+0; 2.92525e-1;
264    1.05871e+0; 2.97064e-1;
265    1.06781e+0; 3.01602e-1;
266    1.07692e+0; 3.06141e-1;
267    1.08602e+0; 3.09545e-1;
268    1.09513e+0; 3.14084e-1;
269    1.10423e+0; 3.18622e-1;
270    1.11333e+0; 3.23161e-1;
271    1.12244e+0; 3.27132e-1;
272    1.13154e+0; 3.31104e-1;
273    1.14065e+0; 3.35642e-1;
274    1.14975e+0; 3.40181e-1;
275    1.15886e+0; 3.44152e-1;
276    1.16796e+0; 3.48124e-1;
277    1.17707e+0; 3.52095e-1;
278    1.18617e+0; 3.56067e-1;
279    1.19527e+0; 3.60605e-1;
280    1.20438e+0; 3.64009e-1;
281    1.21348e+0; 3.68548e-1;
282    1.22259e+0; 3.71952e-1;
283    1.23169e+0; 3.75923e-1;
284    1.24080e+0; 3.79895e-1;
285    1.24990e+0; 3.83299e-1;
286    1.25901e+0; 3.87837e-1;
287    1.26811e+0; 3.91241e-1;
288    1.27721e+0; 3.95213e-1;
289    1.28632e+0; 3.99184e-1;
290    1.29542e+0; 4.02588e-1;
291    1.30453e+0; 4.05992e-1;
292    1.31363e+0; 4.10531e-1;
293    1.32274e+0; 4.13935e-1;
294    1.33184e+0; 4.17339e-1;
295    1.34095e+0; 4.21310e-1;
296    1.35005e+0; 4.24714e-1;
297    1.35915e+0; 4.28118e-1;
298    1.36826e+0; 4.31522e-1;
```

```
299    1.37736e+0; 4.35494e-1;
300    1.38647e+0; 4.38898e-1;
301    1.39557e+0; 4.42302e-1;
302    1.40468e+0; 4.45706e-1;
303    1.41378e+0; 4.49110e-1;
304    1.42289e+0; 4.52514e-1;
305    1.43199e+0; 4.55918e-1;
306    1.44109e+0; 4.59322e-1;
307    1.45020e+0; 4.62726e-1;
308    1.45930e+0; 4.66130e-1;
309    1.46841e+0; 4.69534e-1;
310    1.47751e+0; 4.72371e-1;
311    1.48662e+0; 4.76342e-1;
312    1.49572e+0; 4.79179e-1;
313    1.50483e+0; 4.82583e-1;
314    1.51393e+0; 4.85419e-1;
315    1.52303e+0; 4.89391e-1;
316    1.53214e+0; 4.92227e-1;
317    1.54124e+0; 4.95064e-1;
318    1.55035e+0; 4.98468e-1;
319    1.55945e+0; 5.01305e-1;
320    1.56856e+0; 5.04141e-1;
321    1.57766e+0; 5.07546e-1;
322    1.58677e+0; 5.10950e-1;
323    1.59587e+0; 5.13786e-1;
324    1.60497e+0; 5.16623e-1;
325    1.61408e+0; 5.19460e-1;
326    1.62318e+0; 5.22296e-1;
327    1.63229e+0; 5.25700e-1;
328    1.64139e+0; 5.28537e-1;
329    1.65050e+0; 5.31374e-1;
330    1.65960e+0; 5.34778e-1;
331    1.66871e+0; 5.37614e-1;
332    1.67781e+0; 5.40451e-1;
333    1.68691e+0; 5.42720e-1;
334    1.69602e+0; 5.46124e-1;
335    1.70512e+0; 5.48961e-1;
336    1.71423e+0; 5.51798e-1;
337    1.72333e+0; 5.54634e-1;
338    1.73244e+0; 5.57471e-1;
339    1.74154e+0; 5.60308e-1;
340    1.75065e+0; 5.62577e-1;
341    1.75975e+0; 5.65414e-1;
342    1.76885e+0; 5.68251e-1;
343    1.77796e+0; 5.71087e-1;
344    1.78706e+0; 5.73924e-1;
345    1.79617e+0; 5.76193e-1;
346    1.80527e+0; 5.79030e-1;
347    1.81438e+0; 5.81299e-1;
348    1.82348e+0; 5.84136e-1;
349    1.83259e+0; 5.86973e-1;
350    1.84169e+0; 5.89809e-1;
351    1.85079e+0; 5.92079e-1;
352    1.85990e+0; 5.94348e-1;
353    1.86900e+0; 5.97185e-1;
354    1.87811e+0; 5.99454e-1;
355    1.88721e+0; 6.02291e-1;
356    1.89632e+0; 6.04560e-1;
357    1.90542e+0; 6.07397e-1;
358    1.91453e+0; 6.09666e-1;
359    1.92363e+0; 6.12503e-1;
360    1.93273e+0; 6.14772e-1;
```

```
361    1.94184e+0; 6.17042e-1;
362    1.95094e+0; 6.19311e-1;
363    1.96005e+0; 6.22148e-1;
364    1.96915e+0; 6.24417e-1;
365    1.97826e+0; 6.26686e-1;
366    1.98736e+0; 6.28956e-1;
367    1.99647e+0; 6.31225e-1;
368    2.00557e+0; 6.33494e-1;
369    2.01467e+0; 6.35764e-1;
370    2.02378e+0; 6.38600e-1;
371    2.03288e+0; 6.40870e-1;
372    2.04199e+0; 6.43139e-1;
373    2.05109e+0; 6.45408e-1;
374    2.06020e+0; 6.47678e-1;
375    2.06930e+0; 6.49947e-1;
376    2.07841e+0; 6.52216e-1;
377    2.08751e+0; 6.54486e-1;
378    2.09661e+0; 6.56188e-1;
379    2.10572e+0; 6.58457e-1;
380    2.11482e+0; 6.60727e-1;
381    2.12393e+0; 6.62996e-1;
382    2.13303e+0; 6.65265e-1;
383    2.14214e+0; 6.67535e-1;
384    2.15124e+0; 6.69237e-1;
385    2.16035e+0; 6.71506e-1;
386    2.16945e+0; 6.73775e-1;
387    2.17855e+0; 6.75477e-1;
388    2.18766e+0; 6.77747e-1;
389    2.19676e+0; 6.80016e-1;
390    2.20587e+0; 6.81718e-1;
391    2.21497e+0; 6.83987e-1;
392    2.22408e+0; 6.86257e-1;
393    2.23318e+0; 6.87959e-1;
394    2.24229e+0; 6.90228e-1;
395    2.25139e+0; 6.91930e-1;
396    2.26049e+0; 6.94199e-1;
397    2.26846e+0; 6.94578e-1];
398
399    ndata=size(diamlung,1);
400
401    lungdiam=[];
402    diam=[];
403
404    for i=1:ndata
405        if mod(i,2)==1
406            lungdiam(end+1)=diamlung(i); %abscess along the chamber axis
407        else
408            diam(end+1)=diamlung(i); %diameter
409        end
410    end
411    lungdiam=lungdiam';
412    diam=2*diam';
413
414    %finding the index to divide the cooling system at the throat
415    [dgola,igola]=min(interp1(lungdiam,diam,lung));
416    Tl(igola)=T1;
417    tw1=tw;
418    %cycle from the exit of the nozzle to the nozzle's throat
419    while flag==1
```

```
420        tw1=tw1+0.001*tw1;
421        tsw1=tw1;
422        for i=igola:n-1
423            d=interp1(lungdiam,diam,lung(i)); %interpolated diameter
424            circ=pi*d;
425            circ=circ-tsw1*nc;
426            h=lung(i+1)-lung(i);   %lenght considered for the analysis
427            A=circ*h;
428            bduct=circ/nc;
429            hduct=bduct/2;
430            Aduct=hduct*bduct; %duct area
431            dduct=4*Aduct/(2*(bduct+hduct)); %hydraulic diameter
432            hl=0.023*c*p/Aduct*(dduct*p/Aduct/mu)^(-0.2)*(mu*c/kl)^(-2/3);
433            Tl(i+1)=(Twg(i+1)+p*c*(Tl(i))*(tw1/kw+1/hl)/A)/(1+p*c*(tw1/kw+1/hl)/A);
434        end
435        if abs(Tl(end)-T2)<tol
436            flag=0;
437        end
438    end
439
440    tw2=tw;
441    flag=1;
442
443    %cycle from the nozzle's throat to the starting of the chamber
444    while flag==1
445        tw2=tw2+0.001*tw2;
446        tsw2=tw2;
447        for i=igola:-1:2
448            d=interp1(lungdiam,diam,lung(i)); %interpolated diameter
449            circ=pi*d;
450            circ=circ-tsw2*nc;
451            h=lung(i)-lung(i-1);   %lenght considered for the analysis
452            A=circ*h;
453            bduct=circ/nc;
454            hduct=bduct/2;
455            Aduct=hduct*bduct; %duct area
456            dduct=4*Aduct/(2*(bduct+hduct)); %hydraulic diameter
457            hl=0.023*c*p/Aduct*(dduct*p/Aduct/mu)^(-0.2)*(mu*c/kl)^(-2/3);
458            Tl(i-1)=(Twg(i+1)+p*c*(Tl(i))*(tw2/kw+1/hl)/A)/(1+p*c*(tw2/kw+1/hl)/A);
459        end
460        if abs(Tl(1)-T2)<tol
461
462            flag=0;
463        end
464    end
465
466    %% graphic temperature as a function of position
467    plot(lung,Tl);
468    xlabel('Thrust chamber position [m]')
469    ylabel('Coolant temperature [K]')
```

RaptorInjector.m

```matlab
1    clear all
2    close all
3    clc
4    %% Data
5    P_C = 30000000; % Combustion Chamber Pressure 300 bar
6    OF = 3.4; % Mixing Ratio
7    Qtot = 681.89; % Total Feed
8    rhoF = 143.50; % Fuel Rich Density
9    rhoO = 316.21; % Oxidizer Rich Density
10   rhoMIX = (OF*rhoO + rhoF)/(1+OF); % Mixed Fluid Density
11   %% Number of orifices between injector chamber and combustion chamber
12   DeltaP1 = 0.1*P_C; % Pressure variation between combustion chamber and injector chamber
13   Cd1 = 0.45; % Discharge Coefficient for "Short Tube with Spiral Effect" with
14   % that Diameter
15   D_I = 0.004; % Diameter of the holes (chosen)
16   A_1_H_I = pi*D_I^2/4; % Area of one single hole
17   A_H_I = Qtot/(Cd1*sqrt(2*rhoMIX*DeltaP1)); % Area of all the holes
18   N_I = ceil(A_H_I/A_1_H_I); % Number of holes
19   %% Feed of a single injector
20   Q_I = Qtot/N_I;
21   Q_F = Q_I/(1+OF); % Fuel Feed inside a single injector
22   Q_O = Q_I - Q_F; % Oxidizer Feed inside a single injector
23   %% Area of the holes of Fuel and Oxidizer
24   P_I = P_C + DeltaP1; % Injector Chamber Pressure
25   DeltaP2 = 0.05*P_I; % Pressure variation between inlet feed and injector chamber
26   Cd_F = 0.9; % Discharge Coefficient for "Short Tube with Rounded Entrance" for Fuel
27   Cd_O = 0.8; % Discharge Coefficient for "Short Tube with Conical Entrance" for Oxidizer
28   A_1_H_F = Q_F/(Cd_F*sqrt(2*rhoF*DeltaP2))/2; % Divided per 2 because we suppose
29   % a 2:1 ratio between the hole of the OX and the F
30   D_1_H_F = sqrt(4*A_1_H_F/pi); % The diameter is coherent with the Cd of Fuel chosen
31   A_1_H_O = Q_O/(Cd_O*sqrt(2*rhoO*DeltaP2));
32   D_1_H_O = sqrt(4*A_1_H_O/pi); % The diameter is coherent with the Cd of Oxidizer chosen
33   %% Fluid velocity and dynamic pressure drop
34   u_F = Cd_F*sqrt(2*DeltaP2/rhoF);
35   u_O = Cd_O*sqrt(2*DeltaP2/rhoO);
36   u_MIX = Cd1*sqrt(2*DeltaP1/rhoMIX);
37   DP_dyn_F = rhoF*u_F^2/2;
38   DP_dyn_O = rhoO*u_O^2/2;
39   DP_dyn_MIX = rhoMIX*u_MIX^2/2;
```